WGS KINETICS OVER Pt-BASED TRIMETALLIC CATALYST UNDER REALISTIC CONDITIONS

by

Gizem Yumru

B.S., Chemical Engineering, Boğaziçi University, 2014

Submitted to the Institute for Graduate Studies in
Science and Engineering in partial fulfillment of
the requirements for the degree of
Master of Science

Graduate Program in Chemical Engineering
Boğaziçi University
2017

to Hayal

ACKNOWLEDGEMENTS

Firstly, I would like to express my sincere thanks to my thesis supervisor Prof. Ahmet Erhan Aksoylu for his support, guidance, patience, motivation and encouragement. It was a priviledge to work with him since I learned a lot from his wisdom and expertise in catalysis, reaction engineering.

I would like to express my sincere appreciations for the members of thesis committee, Prof. Hüsnü Atakül and Assoc. Prof. Hasan Bedir, for accepting to be a member of the thesis committee, devoting their valuable time to read and comment on my thesis.

I wish to express my sincere gratitude to Dr. Burcu Selen Çağlayan who deserve special thanks for her excellent guidance, willing to help and give her best suggestions throughout my work.

I would like to thank my dearest and lovely friends Pelin Su Bulutoğlu, Ahmet Coşgun and Zeynep Gülsoy for sharing all the good and bad moments with me and for giving me continuous encouragement and friendship. Deepest thanks to Fuat Alanat for his encouragement, understanding and continuous support on any matter all these years.

Very special thanks to Melek Selcen Başar and Merve Eropak for her everlasting help and guidance throughout my work. I also wish to express my gratitude to all members of KB 411/A. I was very lucky to work with the CATREL team and thus I would like to thank all team members.

Cordial thanks for Bilgi Dedeoğlu for his technical assistance and also Melike Gürbüz, Başak Ünen and Yakup Bal for their friendly help.

I wish to thank my family for all their support, patience and encouragement throughout my life. Their endless love and trust in me was what made me motivated all the time. Finally, very special thanks go to Hayal Çeliksoy for being my nephew.

Financial support for this study was provided by TÜBİTAK through project 214M170. The financial support provided for lab infrastructure by Republic of Turkey Ministry of Development through project 2016K121160 is greatly acknowledged.

ABSTRACT

WGS KINETICS OVER Pt-BASED TRIMETALLIC CATALYST UNDER REALISTIC CONDITIONS

The aim of this study is to obtain a reliable power law type kinetic expression under realistic conditions for water-gas shift reaction over 1Pt-0.5Re-1V/CeO_2 catalyst to be used in designing the WGS unit of a small scale fuel processor. In this content, 1Pt-0.5Re-1V/CeO_2 catalyst was prepared using incipient-to-wetness impregnation method and the preliminary kinetic tests were conducted to determine kinetically controlled and mass transfer limitations free experimental conditions. The kinetic experiments were performed at 350 °C and atmospheric pressure with S/C feed ratio ranging from 15 to 45. 17 pairs of kinetic experiments were conducted according to an experimental design having partial pressures of carbon monoxide, steam, hydrogen, carbon dioxide and methane, and residence time, W/F, as the parameters. Experimental rate data were used to estimate kinetic parameters of the power-law kinetic model by using the method of initial rates. WGS reaction orders were estimated as 0.82, 0.31, -0.29 and -0.35 for carbon monoxide, steam, hydrogen and carbon dioxide, respectively, by using non-linear regression analysis in MATLAB^{TM} within $\pm$6% error margin. Results indicated that the reaction rate increased with an increase in the concentration of CO and H_2O in the feed stream, while it decreased slightly with the addition of H_2 and CO_2. In addition, the effect of methane presence in the feed on WGS kinetics was investigated, and the kinetic reaction rate was found to be practically independent of the concentration of CH_4 in the feed stream as there was no change in the predicted reaction orders of CO, steam, H_2 and CO_2 in the absence and presence of methane term in the rate expression. The apparent activation energy and the frequency factor were calculated as 28.21 kJ mol^{-1} and 29.09 μmol $mgcat^{-1}$ s^{-1} $kPa^{-0.49}$, respectively in a temperature range of 300-350 ºC.

ÖZET

GERÇEK ŞARTLAR ALTINDA Pt-BAZLI ÜÇ METALLİ KATALİZÖRÜN WGS KİNETİĞİ

Bu çalışmanın amacı, gerçekçi besleme koşulları altında su-gaz değişimi reaksiyonu için küçük ölçekli yakıt işlemcisinin WGS ünitesinin tasarımında kullanılmak üzere 1Pt-0.5Re-1V/CeO_2 katalizörü üzerinde güvenilir bir üssel hız denklemi elde etmektir. Bu kapsamda, 1Pt-0.5Re-1V/CeO_2 katalizörü *incipient-to-wetness* empregnasyon yöntemi kullanılarak hazırlanmış ve kütle transferi sınırlamaları olmayan deneysel koşulları belirlemek için ön kinetik testler yapılmıştır. Kinetik deneyler buhar/karbon oranı 15 ile 45 arasında değişen aralıkta 350 °C'de ve atmosfer basıncında gerçekleştirilmiştir. 17 çift deney karbonmonoksit, buhar, hidrojen, karbondioksit ve metanın kısmi basınçları ve reaktörde kalma süresi değiştirilerek yürütülmüştür. Deneysel hız verileri, başlangıç hız yöntemi kullanılarak üssel hız denkleminin kinetik parametrelerini tahmin etmek için kullanılmıştır. WGS reaksiyon mertebeleri doğrusal olmayan bağlanım yöntemi kullanılarak %6 hata payı içinde sırasıyla karbonmonoksit, buhar, hidrojen ve karbondioksite göre 0.82, 0.31, -0.29 ve -0.35 olarak tahmin edilmiştir. Reaksiyon hızı, besleme akışında CO veya H_2O konsantrasyonundaki bir artış ile artarken, besleme akışına H_2 ve CO_2 eklenmesiyle nispeten azalmıştır. Buna ek olarak, besleme akışındaki metan varlığının WGS kinetiği üzerindeki etkisi araştırılmış ve hız ifadesinde metan teriminin varlığında ve yokluğunda, CO, buhar, H_2 ve CO_2'nin öngörülen reaksiyon mertebelerinde herhangi bir değişiklik olmadığı için kinetik reaksiyon hızının, besleme akışındaki CH_4 konsantrasyonundan bağımsız olduğu bulunmuştur. Görünür aktivasyon enerjisi ve frekans faktörü 300-350 ºC sıcaklık aralığında sırasıyla 28.21 kJ mol^{-1} ve 29.09 μmol $mgcat^{-1}$ s^{-1} $kPa^{-0.49}$ olarak hesaplanmıştır.

TABLE OF CONTENTS

LIST OF FIGURES

LIST OF TABLES

LIST OF SYMBOLS

E_A	Activation Energy
$f_{i,in}$	Molar flow rate of species i in the feed stream
$f_{i,out}$	Molar flow rate of species i in the product stream
F	Flow rate
k	Rate constant
k_0	Pre-exponential factor
K_{eq}	Equilibrium constant
m_{cat}	Catalyst weight
P	Pressure
r	Reaction rate
R	Universal gas constant
T	Temperature
vol	Volume
W_{cat}	Catalyst weight
wt	Weight
X	Conversion
α	Reaction order of carbon monoxide
β	Reaction order of steam
β’	Factor of reversible reaction
δ	Reaction order of hydrogen
γ	Reaction order of carbon dioxide
ε	Reaction order of methane
ΔH°_{298}	Standard enthalpy of reaction

LIST OF ACRONYMS/ABBREVIATIONS

ATR	Autothermal Reforming
CATREL	Catalysis and Reaction Engineering Laboratory
DI	Deionized
DRIFT	Diffuse Reflectance Infrared Fourier Transform Spectroscopy
FC	Fuel Cell
FP	Fuel Processor
FTIR	Fourier Transform Infrared Spectroscopy
GC	Gas Chromatograph
GDC	Gadolinium Doped Ceria
GHSV	Gas Hourly Space Velocity
HPLC	High Performance Liquid Chromatography
HTS	High Temperature Shift
ID	Inner Diameter
LTS	Low Temperature Shift
MFC	Mass Flow Controller
OD	Outer Diameter
OSC	Oxygen Storage Capacity
OSR	Oxidative Steam Reforming
PEM	Proton Exchange Membrane
PEMFC	Proton Exchange Membrane Fuel Cell
PGM	Platinum Group Metal
PID	Proportional Integral Derivative
POX	Partial Oxidation
PrOX	Preferential Oxidation
RWGS	Reverse Water Gas Shift
SR	Steam Reforming
SS	Stainless Steel
TCD	Thermal Conductivity Detector
TOF	Turn-over Frequency

TOS	Time-on-stream
TOX	Total Oxidation
WGS	Water-Gas Shift

1. INTRODUCTION

Fossil fuels, primarily coal, fuel oil or natural gas, are the dominant fuels satisfying the global energy demand; they are widely used as they provide a storable, convenient, transportable, and energy-dense form of chemical energy. However, combustion of fossil fuels results in greenhouse gases, such as carbon dioxide, methane and nitrous oxide, which are widely accepted as the reason of global warming. Therefore, researchers have focused on finding alternative energy sources that reduces the release of CO_2 and the other GHG gases including methane (Sathre, 2014).

Hydrogen has been considered as a future energy carrier and it is a perfect candidate to satisfy a plausible fraction of the global energy demand as it can be utilized through efficient and environmentally friendly routes. Hydrogen can be produced through biomass gasification, hydrothermal liquifaction or electrolysis of water, but the common method is steam reforming of hydrocarbons since the fully renewable routes are not economically feasible yet. In foreseeable future, non-intermittent routes of decentralized and dispersed energy production, which supports enhanced use of flow-limited renewable routes, like sun and wind energy, via providing base-load will be of primary concern. The proliferation of smart grid distribution systems, enabling each small-scale energy consumer can also become a producer as long as they produce excessive of their need, accelerates the transition from centralized to decentralized energy production. One of the most widely accepted routes of decentralized non-intermittent energy production at small scale, like in houses, apartments, small business, is Fuel Processor-PEM Fuel Cell (FP-PEMFC) systems for which the PEM-grade hydrogen is produced on site via catalytic routes from hydrocarbons. As there is still technological hurdles and safety concerns in hydrogen storage, the use of fuel processors for on-site hydrogen production is a viable option. Fuel processors convert a hydrocarbon into hydrogen rich reformate, having CO concentration in 100-200 ppm range, feed for the PEM fuel cells. Fuel cell technology has the potential of well-proliferated use in the near future owing to its high efficiency in energy production. Among fuel cell types, polymer electrolyte membrane fuel cells are attractive for many applications, especially of small-scale, as they operate at low temperature and have high power density (Ogden, 1999; O'Hayre *et al*., 2009; Perez *et al*., 2014).

In fuel processors, 3 catalytic reactions occur in series: (i) reforming of hydrocarbons; (ii) water-gas shift reaction (iii) preferential carbon monoxide oxidation. As a result of reforming, besides hydrogen, some other gases such as CO, CO_2, H_2O, CH_4 and other hydrocarbons are formed. In case of small scale on site electricity production through the combined use of FP-PEMFC, CO amount in the reformate must be reduced in order to prevent poisoning of the platinum-based anode of PEMFC for guaranteeing stable operation. The role of the WGS reactor in the fuel processors is to provide a primary CO clean-up step and also acts as a secondary reaction to produce hydrogen (LeValley *et al*., 2014).

Water-gas shift reaction, first reported in 1888, is a well-known process used in chemical industry for the production of methanol, ammonia, hydrogen and hydrocarbons. For hydrogen production in a fuel processor, the main purpose of WGS reaction is to decrease the amount of carbon monoxide and simultaneously increase the hydrogen content of the reformate. WGSR is a reversible moderately exothermic reaction and so CO conversion is limited at high temperatures by thermodynamic equilibrium (Mond and Langer, 1888; Ratsanamy and Wagner, 2009).

In the industrial applications utilizing conventional WGS catalysts, the WGS reaction is carried out in two serial adiabatic stages, namely the high temperature shift followed by low temperature shift since the reaction is kinetically favored at high temperatures and thermodynamically favored at low temperatures. In the high temperature stage, iron/chromium based catalysts are preferred whereas in the low-temperature stage, copper/zinc based catalysts are used. The carbon monoxide concentration of the high temperature WGS product ranges between 2 and 3 vol.% depending on the feed composition whereas the low temperature WGS product contains between 0.05 vol.% for large scale systems, and 0.3-1 vol.% for small scale applications. However, two-stage systems are not economically feasible for fuel cell type operations (Kolb, 2008). Additionally, the use of iron/chromium and copper/zinc based conventional catalysts in the WGS unit of the fuel processor is not suitable due to their thermodynamic and kinetic limitations, pyrophoric structure, detailed activation procedures and long pre-conditioning requirements. Therefore, stable, active, poison resistant and non-pyrophoric platinum

group metal (PGM) based catalysts must be designed and developed for WGS unit of fuel processors (Çağlayan *et al*., 2009; Gonzalez *et al*., 2010).

Recent research has focused on the development of a suitable WGS catalyst which is stable, active, non-pyrophoric, poison resistant and robust in case of rapid shut-down/start-up conditions. In small scale fuel processors, single stage WGS unit operating at HTS-LTS transition temperature range, i.e. 250-400 °C, is preferred. In WGS reaction, both the support and the metal play essential roles in the activity and stability of the catalyst. Noble metal based catalysts supported on CeO_2, ZrO_2 and TiO_2 have been shown to be promising to accomplish this goal (Çağlayan *et al*., 2009; Franchini *et al*., 2012).

In order to design, construct and control an efficient FP, reliable kinetic expressions must be known for each of its catalytic reactions. In the current study, the aim was to obtain a reliable kinetic expression for WGS reaction over Pt-Re-V/CeO_2 catalyst, which have been proven to have high WGS performance in realistic conditions. Kinetic experiments were conducted for different partial pressures of reactants and residence times. The kinetic parameters of the power-law type rate equation were determined by using non-linear regression analysis in MATLAB™.

Chapter 2 contains literature survey including information about hydrogen production, fuel processors, and followed by detailed information about FP reactions, active and selective catalysts for WGS reaction and also kinetic expressions for WGS reaction. The experimental systems and procedures used in the present study are presented in Chapter 3. The results obtained in the experiments and related discussions can be found in Chapter 4. Finally, Chapter 5 includes the conclusions attained from the present study and recommendations for future work.

2. LITERATURE SURVEY

2.1. Fuel Cell and Fuel Processor Technology

A fuel cell is an electrochemical device which generates electricity by converting hydrogen through a chemical reaction. Fuel cells, which are highly efficient in energy conversion, are an alternative for clean energy production in recent years due to less/no harmful emissions since using hydrogen as a fuel provides only water emisson (Dönitz, 1998).

Proton exchange membrane fuel cells are considered as the most promising fuel cell type for small scale applications for several reasons. First, their power density is very high particularly in pressurized systems. In addition, since the pressure difference between the anode and the cathode is very large owing to its solid polymer electrolyte, system operation is quite easy even in pressurized system. Moreover, a wide variety of materials can be adopted for cell components due to its low operating temperature (80 °C), compared with other types of fuel cells. However, at low temperatures, PEMFCs are very susceptible to carbon monoxide poisoning (Okada and Yokoyama, 2001).

The ideal fuel for PEMFCs is pure hydrogen, with less than 40 ppm carbon monoxide, owing to its high reactivity at the anode. Hydrogen fuel is not found in nature, so it is an energy carrier rather than an energy source. Thus, nearly CO-free and sulfur-free gas feed must be produced. Most studies have been focused on the design of on-site hydrogen generation for use in PEMFCs since the major challenge for small-scale fuel cell is storage of hydrogen fuel (Palma *et al*., 2017). Many studies have focused on small-scale fuel processor technologies as components of fuel cell systems. The optimum solution could be to transport liquid fuels having high energy densities and convert them to a hydrogen rich gas (reformate) via fuel processor. The combined FP-PEMFC system is the most promising option for both vehicular and small-scale stationary applications (Gökaliler *et al*., 2008; Holladay and Wang, 2015).

A fuel processor consists of three catalytic reaction units in series: a reforming unit to produce hydrogen rich synthesis gas from hydrocarbons, a water-gas shift unit to convert CO in further H_2, and a preferential oxidation unit to decrease CO concentration to ppm levels. There are several methods for hydrocarbon reforming, namely steam reforming (SR), partial oxidation (POX), and oxidative steam reforming (OSR). Fuel processors for PEMFCs must generate a hydrogen rich gas with less than 40 ppm CO concentration since CO poisons the catalysts and the Pt anode of the PEM type fuel cells, when its concentration is greater than 40 ppm (Çağlayan *et al*., 2009).

2.1.1. Reforming Reaction

The reforming unit converts hydrocarbon fuels into hydrogen-rich synthesis gas by applying heat. Steam reforming is highly endothermic and conducted at high reaction temperatures (above 700 °C). Nickel is known to be catalytically active metal in the steam reforming process since Ni promoted catalysts are conventional, cheap and efficient for large scale hydrogen production although Ni is less active compared with some noble metals and more prone to deactivation. Since the reforming reaction requires high temperature, coke formation can be observed on catalyst surface. In order to overcome that problem water should be added in sufficient amounts. Main advantage of SR to other hydrogen production routes is the high H_2 yield. However, SR is not suitable for on-site FP-FC applications due to the need of large reactor size. The general equations of SR reactions are given in Equation 2.1 and 2.2 (Rostrup-Nielsen, 1984; Trimm and Önsan, 2001; LeValley *et al*., 2014).

$$C_mH_{2n} + mH_2O \rightarrow mCO + (m+n)H_2 \quad (2.1)$$

$$C_mH_{2n} + 2mH_2O \rightarrow mCO + (2m+n)H_2 \quad (2.2)$$

Partial oxidation reaction is highly exothermic and converts the hydrocarbon fuel into a mixture of H_2 and CO, instead of CO_2 and H_2O as in total oxidation (TOX) reaction. In POX reaction, hydrogen yield is lower compared to steam reforming. Depending on the catalyst, the residence time and the amount of oxidant in the feed, POX (Equation 2.3) reaction turns to TOX (Equation 2.4). Unlike total oxidation, partial oxidation reaction

uses lower stoichiometric oxygen with respect to the hydrocarbon fuel (Hu and Ruckenstein, 2004).

$$C_mH_{2n} + (\frac{1}{2}m)O_2 \rightarrow mCO + nH_2 \quad (2.3)$$

$$C_mH_{2n} + (m+\frac{1}{2}n)O_2 \rightarrow mCO_2 + nH_2O \quad (2.4)$$

In order to provide energy efficiency and overcome the difficulties of SR and POX, the endothermic SR and exothermic POX of hydrocarbons are coupled, and named as oxidative steam reforming. OSR reduces coke formation and also increases hydrogen yield. In OSR, oxygen to carbon ratio, steam to carbon ratio and temperature are important parameters since these parameters affect H_2 and CO concentrations in product stream (Shekhawat *et al*., 2011).

2.1.2. Water-Gas Shift Reaction

WGS is an important step for a fuel processor since it produces hydrogen, also reduces CO levels in the reformate gas stream down to 0.5-1%. The reaction is thermodynamically favored at low temperatures and kinetically favored at high temperatures. Therefore, conventionally WGS reaction is conducted in two serial reactors, namely high temperature shift (HTS) and low temperature shift (LTS). HTS is conducted over Fe_2O_3/Cr_2O_3 catalysts at 310-450 °C temperature interval, while LTS is carried out over $Cu/ZnO/Al_2O_3$ catalysts at 200-250 °C (Smith *et al*., 2010).

$$CO + H_2 \leftrightarrow CO_2 + H_2 \qquad \Delta H^0_{298} = -41.1 kj/mol \quad (2.5)$$

2.1.3. Preferential Oxidation Reaction

PrOX reaction reduces the CO level from 0.5-1% to below 40 ppm. Complete removal of CO is an essential requirement for hydrogen used as a fuel to PEM fuel cells. The PrOX catalyst should be very selective, such that instead of oxidizing the highly

concentrated H_2 in the feed, it should oxidize CO. This can be adjusted by carefully controlling the reaction temperature. Almost 100% CO conversion is achieved at low temperature 100-150 °C. Pt is reported to be a promising active metal to be used in PrOX catalysts (Ratnasamy *et al*., 2004).

$$CO + \frac{1}{2}\,O_2 \rightarrow CO_2 \qquad \Delta H^0_{298} = -283kj/mol \tag{2.6}$$

$$H_2 + \frac{1}{2}O_2 \rightarrow H_2O \qquad \Delta H^0_{298} = -242kj/mol \tag{2.7}$$

2.2. WGS Catalysts

The water gas shift is a crucial reaction for fuel processing, since it provides not only CO reduction in reformate but also an increase in hydrogen concentration. The WGS reaction is an equilibrium-controlled and moderately exothermic reaction.

The industrial scale water gas shift reaction is carried out in two adiabatic stages consisting of high temperature shift followed by low temperature shift reactors. Iron-chromium catalysts are used only in HTS because they lose their activity at lower temperature. On the other hand, copper-zinc based catalysts are used as LTS catalysts, and they are not suitable for operation at higher temperature as they have tendency to sintering. For fuel processor applications, the requirements of WGS catalysts are quite different from the conventional iron-chromium and copper-zinc based catalysts. The two HTS and LTS catalysts are pyrophoric in their activated form, so there is a much research to develop a single stage non-pyrophoric WGS catalyst (Smith *et al*., 2010).

Conventional water gas shift catalysts cannot be used in small scale fuel processors owing to their pyrophoric structure, long pre-conditioning requirements, restrictions in volume, weight and cost. Moreover, fuel processor-fuel cell systems undergo too many shut-down/start-up operations leading severe deactivation problem (Guo *et al*., 2009; Roh *et al*., 2011). Krekel *et al*. (2016) have conducted their study on catalyst deactivation under steady-state and shut-down/start-up operations. The reason behind the deactivation was suggested to be carbon deposition, owing to the occurrence of higher hydrocarbons in the

reformate. As severe catalyst deactivation was detected during shut-down/start-up operations compared to that during steady state operation of fuel processors, developing new shut-down and start-up strategies is of crucial importance.

The activity of Cu-based catalysts with different supports, which are ceria, ceria-zirconia and ceria-titania, was investigated by Pradhan *et al*. (2009) via changing gas hourly space velocity. They have found that the higher loading of CuO on oxide supports could result in bigger particles, which leads to a decrease in the activity. Therefore an optimum loading of 10% wt. was chosen. Their results indicated that $CuO\text{-}CeO_2\text{-}ZrO_2$ and $CuO\text{-}CeO_2$ showed better performance than $CuO\text{-}CeO_2\text{-}TiO_2$, and the activity order was found as $CuO\text{-}CeO_2\text{-}ZrO_2 > CuO\text{-}CeO_2 > CuO\text{-}CeO_2\text{-}TiO_2$.

The Gunawardana *et al*. (2009) have investigated the performance of the WGS reaction in the reaction temperature range of 150–360 °C over copper–based catalysts in which copper loadings change between 20 to 90% Cu. They found that the WGS activity of Cu-based catalysts supported on ceria increased with copper loadings and 80% copper–ceria catalyst showed the highest performance. The catalysts were stable at medium temperature, but deactivation was obtained with the temperature increase.

Catalyst preparation method significantly affects the catalyst performance. Aguila *et al*. (2013) have compared the activity of Cu/ZrO_2 catalysts in the WGS reaction prepared by a reflux method and by conventional impregnation. The results revealed that the tetragonal phase was required in order to obtain high activity and by using the reflux method tetragonal zirconia was generated. Also, higher particle size of CuO was formed using the reflux method than those obtained using the impregnation method. Therefore, the catalyst activity prepared by reflux was better for the WGS reaction.

The main drawback of Cu-based catalysts is that they are not very stable against oxidizing gases when compared to Pt-, Ru- or Au-based catalysts (Nishimura *et al*., 2010). During the shutdown operation, the catalysts can be exposed to oxygen containing atmosphere, resulting in the oxidation of the active species. Moreover, temperature rise of Cu-based catalysts exposed to air can reach to above 600 °C. This high temperature rise

will result in irreversible catalyst deactivation owing to sintering of the copper species (Liu *et al*., 2012).

Most of the studies were conducted on Pt and Au based catalysts since they were considered as leading candidates to be used in small scale fuel processors. The studies on Au-based WGS catalysts revealed that Au supported on metal oxides show high catalytic activity, especially at low temperatures. Au-based catalysts are commonly used in WGS applications owing to their lower prices compared to Pt-based catalysts although several studies reveal that Pt is very active compared to other precious metals such as Au (Duarte de Farias *et al*., 2008).

Castano *et al*. (2014) have compared the platinum and gold based catalysts behavior for the water gas shift reaction. It was known from the studies that copper-zinc catalysts required safety cautions on air exposure due to its pyrophoricity, so they suggested noble based catalysts such as Pt and Au catalysts instead of copper-zinc. The gold catalysts showed higher conversion when supported on CeFeAl rather than Al_2O_3 regardless of the reaction temperature. The same was valid for platinum catalysts for reaction temperatures below 300 °C. The results showed that at low temperatures gold catalysts were always more active than platinum catalysts, but the reverse was true for temperatures above 200 °C. In addition, Lenite *et al*. (2011) demonstrated that Au catalysts supported on alumina were not so active despite an excellent gold deposition on support.

Reina *et al*. (2015) have studied to increase the efficiency of $Au/CeO_2/Al_2O_3$ based WGS catalysts. They conducted their study by adding transition metals, namely Fe, Cu and Zn. All the transition metals significantly enhanced the WGS performance of the undoped sample since all dopants increased the oxygen storage capacity (OSC) of the ceria-alumina support and, hence led to an increase in reducibility and greater oxygen availability. Among all the dopants, the best result was obtained with Fe since the Au/CeFe/Al sample showed the highest OSC at 250 °C and 350 °C. It was concluded that Fe, Cu and Zn dopants significantly promoted the WGS activity of the $Au/CeO_2/Al_2O_3$ catalyst.

Reina *et al*. (2016) have studied the role of Au, Cu, CeO_2 and their interactions in order to obtaine good catalytic activity. Their studies indicated that the multicomponent

catalysts showed appreciable long-term stability and tolerance towards start-up/shut-down cycles. The water gas shift catalysts must present excellent redox since the WGS reaction is a redox process. It is known from the studies that the oxygen storage capacity is important for redox property. The magnitude of Au-support interaction affects the OSC, enhancing the reduction of catalyst components. Among the gold-based catalysts, the ones rich in copper showed better catalytic activity, and the best result was obtained over Au/Ce2Cu8/Al sample as Cu itself was rather active at low temperature. The multicomponent catalyst (Au/Ce2Cu8/Al) was more stable in both long-term tests and start-up/shut-down cycles since ceria helped to prevent the carbonate formation that were related to the catalysts deactivation.

Liu *et al*. (2013) have investigated the deactivation mechanisms of the Au/CeO_2 catalyst in steady-state and shut-down/start-up conditions in realistic feed at 250 °C. In steady-state operation, the reason of catalyst deactivation is the reduction of the catalyst by H_2 and CO, resulting in weak $Au\text{-}CeO_2$ interaction, which is crucial for WGS activity. On the other hand, in shut-down/start-up operations, the deactivation was attributed to the deposition of the carbonate species, originating from CO_2 and H_2O. It was indicated that by calcining the catalyst, carbonate species can be removed, and 90% of the original activity was reached over the reactivated sample.

Perez *et al*. (2014) have focused on the low temperature water gas shift reaction over ceria promoted nickel catalysts supported on carbon since cerium oxide is commonly used as catalyst support and promoter due to its high oxygen storage capacity and reducibility. They carried out their study by changing ceria loadings such as 10, 20, 30 and 40% wt. Catalysts with 10 and 20wt.% CeO_2 were found as the most active at low temperatures. Small ceria particles with high dispersion led to an enhance in reduction of ceria, which interacts with the nickel particles to different extents. $Ni20CeO_2/C$ catalyst showed the highest activity at low temperature, owing to the synergistic effect between the Ni and CeO_2.

Kam *et al*. (2010) have also focused on the pyrophoricity of Pt based and Cu/ZnO based catalysts through shut-down/start-up operations at the low temperature for WGS reaction. For any of the Pt-based catalysts, no pyrophoricity was observed and Pt/TiO_2

showed the highest activity followed by Pt/CeO_2 and then Pt/ZrO_2. In general, Cu/ZnO-based catalysts were found more active compared to Pt-based catalysts at temperatures between 150 and 300 °C but the deactivation was occurred in all Cu-based catalysts during the shut-down/start-up operations.

In another study conducted by Germani *et al*. (2005), it was proposed that platinum/ceria/alumina catalysts were very active for the WGS reaction in the temperature range from 300 to 400 °C. They have investigated the effect of the amount of platinum and ceria on the catalytic activity and found that the ceria amount did not affect the catalyst activity to a great extent. Moreover, they also studied to develop the platinum/ceria/alumina catalysts on microstructured platelets. They revealed that the catalyst on microstructured platelets were more active compared to the powder samples since the diffusion limitations were observed inside the powder pellets. A better platinum utilization was obtained in catalyst deposited on microstructured platelets.

The catalyst deactivation is a complex process and many factors can affect the deactivation. Liu *et al*. (2005) findings showed that the carbonates were formed on the catalyst surface as a result of shutdown in the reformate, resulting in deactivation and they covered both the surface of ceria and Pt metal surface. It could be said that there was a correlation between the degree of deactivation and the content of carbonates. It is concluded that the carbonate formation resulted in the continuous deactivation of Pt-based catalyst supported on high surface area CeO_2.

Çağlayan *et al*. (2009) have made an investigation on the effect of second metal addition. The water gas shift activity of bimetallic $Pt\text{-}Ni/Al_2O_3$ catalysts was studied at the medium temperatures between 200 and 450 °C. The results showed that $Pt\text{-}Ni/Al_2O_3$ catalysts were highly active and selective for WGS reactions under ideal conditions. In addition, equilibrium conversion could be reached at lower temperatures with the increase in Ni loading.

Zhu *et al*. (2011) have investigated the effects of Na promotion for high water gas shift activity on co-impregnated $Pt–Na/TiO_2$ catalyst having Na loadings in the range 0-10% wt. They found out that there were strong metal-promoter interactions between Pt and

Na metals, which facilitated the reduction of Na promoter. It was stated that the activity was greatly affected by the addition of Na promoter and the optimum result was obtained with 3-4% wt. Na loading.

The effect of zirconia polymorphism over platinum-based catalysts in WGS reaction systems was methodically studied by Franchini *et al*. (2012). The changes in metal dispersion could affect the deactivation of ZrO_2 supported WGS catalysts during reaction. They revealed that zirconia polymorphism determined the catalyst activity, and the monoclinic structure Pt/m-ZrO_2 sample indicated to be significantly more active compared to Pt/t-ZrO_2.

Kalamaras *et al*. (2011) have investigated the effect of Pt particle size, changing between 1.3 and 8 nm, on kinetic and mechanistic aspects of the WGS reaction. It was concluded that the WGS reaction on Pt/CeO_2 at 300 °C governed mostly via the 'redox' mechanism, and to a lesser extent via 'the associative formate with -OH group regeneration' mechanism. Moreover, it was proposed that the change in the particle size slightly affected the TOF (s^{-1}) of WGS, whereas the increase in the particle size increased the specific rate of reaction dramatically.

Çağlayan *et al*. (2011) have made an investigation on the effect of Re addition to Au/ceria catalysts. The results revealed that Au–Re/ceria catalysts showed higher catalytic performance for WGS reaction, especially at high H_2O/CO ratios, owing to beneficial interaction between gold and rhenium particles. In Villar *et al*. (2015) studies, the effect of Re addition into Pt/CeO_2–TiO_2 catalyst on the WGS activity and stability was investigated. They found out that the WGS activity and stability of the Pt/CeO_2–TiO_2 catalyst was markedly effected by the rhenium addition. At first the monometallic Pt/CeO_2–TiO_2 catalyst showed high initial WGS conversion but it deactivated as time progresses. However, the effect of addition of rhenium to Pt/CeO_2–TiO_2 catalysts improved the catalyst stability under WGS conditions. In the case of bimetallic Re-Pt/CeO_2–TiO_2, sintering was observed but to a less extent compared to monometallic case.

The effect of Re addition as a second metal beside a precious metal has been studied by Azzam *et al*. (2007b). They proposed that second metal addition (Re) led to an increase

in stability of Pt/TiO_2, which prevented Pt sintering observed in previous study (Azzam *et al*., 2007a). In addition, they investigated the effect of the support on the catalytic performance and best catalytic activity was obtained over $Pt\text{-}Re/TiO_2$ compared with $TiCeO_2$, $CeZrO_2$, CeO_2, $TiZrO_2$ and ZrO_2. It was assserted that certain Re amount presented in in oxidized form (ReOx), resulting in an improvement in the catalyst activity.

Tepamatr *et al*. (2006) have also investigated Re addition to Cu supported on CeO_2 and gadolinium doped ceria (GDC). It was revealed that Re addition to Cu/GDC considerably enhanced the catalytic performance of copper catalysts. The reason of this improvement was that Re increased the reducibility of the surface ceria. Moreover, Re contributed to reduction of Ce^{4+} to Ce^{3+}. The findings indicated that the bimetallic catalyst 1%Re4%Cu/GDC showed higher activity compared to the monometallic catalysts owing to its electron density transfer between Re, Cu, Ce and Gd, which would occur and led to a reduction of the catalyst surface becoming easier.

Azzam *et al*. (2013) have conducted WGS reaction over $Pt\text{-}Re/TiO_2$ catalyst changing preparation strategies, Pt/Re molar ratios, and metals contents in order to analyze interaction between Pt and Re. They found that the optimum preparation method for WGS activity and stability was the sequential impregnation of Re prior to Pt without intermediate drying and calcination and the highest activity and stability was obtained at Pt:Re molar ratio of unity with 0.5 wt.% Pt content. In addition, ReOx species was partially reduced under the WGS conditions, which provided an additional reaction pathway, in which ReOx was reduced by CO and reoxidized by H_2O and this additional redox route was the major reason for the high activity.

Vanadium oxide has widely been studied in oxidation reactions since it provides high oxygen mobility when it is partially reduced, owing to its capacity of structural defect generation, making vanadium a favorable metal for catalysts used for WGS reaction. (Haber *et al*., 1997). Duarte de Farias *et al*. (2008), have investigated the effect of vanadium addition into Pt/CeO_2 and found that regardless of the amount, it resulted in an enhancement in WGS activity. The incease in WGS reaction rate was seemed to be related with the V–O–Ce bonds.

The effect of vanadia (V_2O_5) addition to Pt/ZrO_2 catalyst for WGS reaction was investigated by Nguyen-Thanh *et al*. (2008). The results revealed that vanadia resulted in an improvement in WGS activity and the optimum catalyst, containing 3 wt.% of vanadia, doubled the reaction rate of the unpromoted Pt/ZrO_2 when the monovanadate was the predominant species. The promoting effect of monovanadate was proposed to be a consequence of enhanced reducibility provided through formation of V–O–Zr bonds.

2.3. WGS Kinetics

Kinetic expressions for WGS reaction on different composition and new catalysts are important to determine the rate of the reaction and hence design the reactors. Both the microkinetic and the empirical approaches can explain the kinetic expressions for WGS reaction.

The detailed chemistry of surface can be analyzed using the microkinetic method. This method provides the reaction order, activation enthalpy and surface coverage. Since the microkinetic method is computationally intensive there is no single mechanism consistent with all experimental observations. In literature two mechanistic paths are largely considered for the WGS reaction: a “redox” and an “associative” mechanism. In redox mechanism, the catalyst surface is oxidized by H_2O, producing H_2 and reduced by CO, converting to CO_2. The associative mechanism is an adsorption – desorption model in which the adsorbed species interact to form an adsorbed intermediate which then decomposes to generate H_2 and CO_2 (Azzam *et al*., 2008; Smith *et al.*, 2010).

The empirical models are expressed in power-law type rate expressions and obtained using experimental results. The power law type model is an easy and computationally lighter way to estimate the rate of reaction. Although power-law type of rate expression does not give a detailed idea about mechanisms of reactions, they are beneficial for prediction of system performance, comparison of different catalysts and designing reactors (Hla *et al*., 2011).

There are many studies on kinetics of WGS reaction over various catalysts for different feed compositions. Most studies were conducted under different conditions so, it is difficult to compare the reaction rates with ones reported in the literature.

Keiski *et al*. (1992) have investigated kinetic parameters of a conventional HTS iron-based catalyst (Fe_2O_3/Cr_2O_3) under realistic feed conditions at temperatures between 300 and 400 °C. Reaction orders with respect to CO an H_2O were found as 0.74 and 0.47, respectively. A small negative value -0.2 of the CO_2 concentration exponent was obtained which indicated the inhibitory effect of CO_2 on the reaction rate. The effect of the H_2 concentration was not found. In another study, Keiski *et al*. (1996) have conducted WGS reaction over Fe_3O_4/Cr_2O_3 catalyst under ideal feed conditions. The kinetics parameters were found as 1.1 and 0.53 with respect to CO and H_2O. These parameters are a little high compared with previous study, which could be derived from the absence of inhibitory effect parameters.

Plaza *et al*. (2016) have carried out their studies employing two commercially available catalysts based on Co-Mo and Fe-Cr at 300 °C. The reaction orders for Fe-Cr based catalyst were estimated as 1.37, 0.23, -0.16 and -0.11 with respect to CO, H_2O, CO_2 and H_2, respectively. Therefore, the reaction rates were increased significantly with increasing CO concentrations. The apparent reaction orders reported in the literature were usually obtained in a sulfur free feed, whereas this study was performed at an H_2S concentration of 100 vol.ppm. The reaction order of the Fe/Cr-based catalyst with respect to H_2S was estimated to be -0.28 whereas sulfur addition affected Co-Mo-based catalyst positively. Boon et al. (2009) also studied the effect of sulphur on WGS kinetics and found that H_2S negatively affected the reaction rate. It was proposed that an increase in the sulphur amount resulted in a decrease in CO_2 reaction order magnitude from -0.60 to -0.10 because adsorption of H_2S would lower the adsorbed amount of CO_2.

Koryabkina *et al*. (2003) have studied the kinetic expression for water–gas shift reaction on Cu-based catalysts under realistic feed conditions for fuel cell applications (7% CO, 8.5% CO_2, 22% H_2O, 37% H_2) at temperature interval of 190-240 °C. The reaction rates were found in per unit of mass of catalyst for different Cu-based catalysts. The industrial $CuO–ZnO–Al_2O_3$ catalyst showed the highest activity on the basis of unit of

mass of catalyst. However, they found that the reaction orders were similar for all catalysts. The kinetic studies performed in this work showed that at 190 °C the WGS reaction on the CuO–ZnO–Al_2O_3 catalyst is of 0.8, 0.8, -0.9 and -0.9 order with respect to CO, H_2O, CO_2, and H_2, respectively. In addition, Ovesen *et al*. (1996) have investigated the reaction orders on CuO–ZnO/Al_2O_3 catalyst. They have conducted their kinetic experiments over Cu/ZnO/Al_2O_3 at similar reaction temperature and partial pressures with Koryabkina *et al*. Their power rate laws were consistent with each other. In both studies, the reaction products (CO_2 and H_2) resulted in strong catalyst inhibition.

Koryabkina *et al*. (2003) have also analyzed the surface mechanism and found that the kinetic model have been a good representation of the surface redox mechanism which showed that reduction of surface oxygen by adsorbed CO is the rate determining step

In another study conducted by Choi and Stenger (2003), the kinetics of the WGS reaction were evaluated over a commercial Sud-Chemie Cu/ZnO/Al_2O_3 catalyst in the temperature range of 120-250 °C under ideal feed conditions with S/C ratio ranging from 0 to 5. The first order dependency for both CO and water was found. Also, the single path redox mechanism and the double site Langmuir–Hinshelwood type rate expression from the adsorptive mechanism fitted the experimental data at good level.

Bunluesin *et al*. (1998) estimated a CO reaction order of 0.3 for ceria layer on α-alumina wafer reaction at 300 °C under ideal feed. Deposition of platinum metal (Pt, Rh and Pd) nanoparticles on these CeO_2 substrates resulted in zero CO reaction order under similar conditions. It was proposed that noble metals strongly adsorbed CO at high partial pressures and lower temperatures, so that an increase in CO partial pressure would not increase the reaction rate owing to high surface coverage. For different catalysts, a first-order dependency of water on the WGS reaction rate has been reported since molecular adsorption of water on metals was weak. It can be concluded that the metal component did not play a significant role for water order.

Kinetic and mechanistic aspects of WGS reaction on Au/CeO_2 catalysts under realistic reaction conditions at 180 °C were studied by Leppelt *et al*. (2006). The reaction orders determined from the slopes of the reaction rate versus ln of partial pressures were

0.5 for CO and water and −0.5 for CO_2 and H_2. Koryabkina *et al*. (2003) determined the reaction orders over a Cu/CeO_2 catalyst at 240 °C under realistic conditions (CO: 5–25 kPa, H_2O: 10–46 kPa, CO_2: 5–30 kPa, H_2: 25–60 kPa), they derived values of 0.9 for CO, 0.4 for water, and −0.6 for CO_2 and H_2, which were close to Leppelt's results. On Au-based catalysts, the steady-state CO_{ad} coverage was rather low compared to Pt-based catalysts under reaction conditions at 180 °C, and an increase of the CO partial pressure affected CO_{ad} coverage positively.

Hilaire *et al*. (2001) have estimated reaction orders on Pd/ceria as approximately zero-order in CO, half-order in H_2O, inverse-first-order in H_2 and inverse-half-order in CO_2. It was concluded that Pd surface almost certainly was saturated with CO at 200-240 °C temperature range, so that the coverage of adsorbed CO was not strongly affected by an increase in the CO pressure. The half-order dependence on H_2O revealed that the rates were partially limited by reoxidation of ceria. However, the reason of dependency for H_2 was uncertain. The dependency could be originated from competitive adsorption with carbon monoxide on the Pd, competition with water for oxidation of reduced ceria or simply a surface equilibrium effect.

A kinetic study of the WGS reaction on a 0.5 wt.% Pt/TiO_2 catalyst has been conducted by Kalamaras *et al*. (2009). They revealed that the reaction rate increased with an increase in the CO or H_2O partial pressures in the feed stream whereas it decreased dramatically with the increase in H_2 concentration. The concentration of CO_2 in the feed stream did not affect the reaction rate. The kinetic reaction orders with respect to CO, H_2O, CO_2, and H_2 were found to be 0.5, 1.0, 0.0 and -0.7, respectively. Many studies proposed that carbon monoxide concentration used in the feed stream determines the CO reaction order. In this work, the reaction order with respect to CO was estimated as 0.5 due to low CO concentrations (1–4 vol.%). Moreover, a first-order dependency of water could be explained that rate was limited by the re-oxidation of support by water. It can be concluded that for low H_2O partial pressures the reaction orders have become zero and first order with respect to CO and H_2O, respectively and an increase in the concentration of H_2O resulted in a progressive increase of the surface concentration of –OH groups. They have explained the negative dependency (-0.7) on H_2 through the competitive adsorption of H_2 with CO.

Azzam *et al*. (2008) have studied the kinetics of the WGS reaction over Re-Pt/TiO_2 catalyst and found that CO adsorption can be ruled out as the rate determining step under feed conditions with high CO concentration at 300 °C. Zero order kinetics observed for CO_2 indicated that desorption of CO_2 from TiO_2 occured fast since Pt did not adsorb CO_2 at this temperature. The carbonates were unstable on TiO_2 at the reaction temperature. Therefore, desorption of CO_2 cannot be considered as rate limiting step. For water, the first order dependency showed that rate was limited by re-oxidation of TiO_2. Unlike Kalamaras *et al*. (2009) opinions about negative dependency of H_2, they did not think that the rate inhibition was due to competitive adsorption between ‘‘H’’ and CO on Pt surface because CO adsorption was known to be much more facile than ‘‘H’’ on Pt. They concluded that hydrogen inhibited the WGS reaction rate over Pt/TiO_2 catalysts by suppressing the formation of OH groups on TiO_2 since the reaction step between adsorbed CO on Pt and OH groups of TiO_2 is the rate-determining step.

Gökaliler *et al*. (2013) have conducted the kinetic studies of 1Au–0.5Re/CeO_2 catalyst at 280–325 °C for realistic reformate streams. WGS reaction orders were estimated as 0.75, 2.0, -0.34 and -0.60 for carbon monoxide, steam, carbon dioxide and hydrogen respectively. The reaction order with respect to H_2O was higher compared to ones reported in the literature. The reason of this difference was considered as the addition of Re to the Au/CeO_2 catalyst, since it was known that high steam content resulted in highest WGS activity over Au–Re/CeO_2 catalyst under realistic feed conditions and the high water activation ability of Re led to high catalytic activity.

Many studies revealed that a zero-order dependency of reaction rate on CO was found over noble metal supported catalyst (Ovesen *et al*., 1992; Bunluesin *et al*., 1998; Hilaire *et al*., 2001; Radhakrishnan *et al*., 2006; Phatak *et al*., 2007; Azzam *et al*., 2008). Jacobs *et al*. (2003) have found the zero reaction order with respect to CO over Pt/CeO_2 at high CO concentrations, whereas at low CO partial pressures the reaction order with respect to CO was found to be of first order, owing to the difference in surface coverages. Moreover, at higher reaction temperatures the reaction rate dependency on CO was expected to be positive (Mhadeshwar and Vlachos, 2005). This was coincided with the results of Jacobs *et al*. (2003) for the Pt/CeO_2 catalyst. They have proposed that at high temperatures the surface coverage of CO was low, and thus caused that the observed

reaction order with respect to CO was 1.0. At low temperatures both Pt-CO and formates were close to their equilibrium adsorption-desorption values.

The kinetic parameters for the WGS reaction on Pt catalysts supported ceria and alumina under realistic feed conditions (7% CO, 8.5% CO_2, 22% H_2O and 37% H_2) in the temperature range of 200–315 °C were estimated by Phatak *et al*. (2007). On the basis of the turnover rate, ceria was found to be a strong promoter for Pt based WGS catalysts. The WGS reaction on the present Pt/TiO_2 catalyst was of -0.03, 0.44, -0.09, and 0.38 order with respect to CO, H_2O, CO_2, and H_2, respectively whereas for the Pt/Al_2O_3 catalyst the reaction orders was found as 0.1, 0.77, -0.08 and -0.46. The difference in H_2O reaction order on alumina and ceria supported catalysts was originated from that different reaction mechanisms might operate on these catalysts. They revealed that the reaction rate dependency on CO_2 over Pt/CeO_2 and Pt/Al_2O_3 catalysts was slightly negative and close to zero, respectively, owing to the very weak interaction of CO_2 with Pt. The apparent reaction order of H_2 close to -0.5 indicated H_2 inhibition of the forward WGS since an increase in the concentration of H_2 caused an increase in the surface coverage of atomic hydrogen.

The effect of rhenium promoter over Pt-based catalysts supported on ceria-zirconia on the WGS reaction rate was also investigated by Radhakrishnan *et al*., (2006). The apparent activation energy value and reaction orders on 1% Pt/CeO_2 were found similar to those reported by Phatak *et al*. (2007). They found that the Re addition to Pt-based catalyst led to a higher reaction order for H_2O and smaller negative orders with respect to CO_2 and H_2.

3. EXPERIMENTAL WORK

3.1. Materials

3.1.1. Chemicals

All of the chemicals used for catalyst preparation are listed in Table 3.1.

Table 3.1. Chemicals used in catalyst preparation.

Chemicals	**Formula**	**Specification**	**Source**	**Molecular Weight (g/mol)**
Ammonium meta-vanadate	NH_4VO_3	99%	Riedel-de Haën	116.98
Aluminum oxide α-phase	α-Al_2O_3	99.9%	Alfa Aesar	101.96
Ammonium perrhenate	NH_4ReO_4	99.999%	Sigma-Aldrich	268.24
Cerium (III) nitrate hexahydrate	$Ce(NO_3)_3 \cdot 6H_2O$	99.99%	Sigma-Aldrich	434.23
Oxalic acid dihydrate	$C_2H_2O_4 \cdot 2H_2O$	98%	Alfa Aesar	126.07
Sodium carbonate	Na_2CO_3	99.9+%	Merck	105.99
Tetraammineplatinum (II) nitrate	$Pt(NH_3)_4(NO_3)_2$	99.995%	Aldrich	387.22
Water	H_2O	Deionized	-	18.02

3.1.2. Gases and Liquids

All of the gases used in this study were supplied by the Linde Group, Gebze, Turkey. The specifications and applications of the liquid and gases used in this study are listed in Table 3.2. and Table 3.3, respectively.

Table 3.2. Specification and application of the liquid used.

Liquid	Formula	Specification	Application
Water	H_2O	Deionized	Aqueous solutions, Reactant

Table 3.3. Specifications and applications of the gases used.

Gas	Formula	Specification	Application
Argon	Ar	99.995%	Inert, GC carrier gas
Carbon dioxide	CO_2	99.995%	Reactant, GC calibration
Carbon monoxide	CO	99.999%	Reactant, GC calibration
Dry air	N_2O_2 mixture	99.998%	GC 6-way pneumatic valve
Hydrogen	H_2	99.995%	Reactant, Reducing agent, GC calibration
Methane	CH_4	99.995%	Reactant, GC calibration

3.2. Experimental Systems

The experimental systems used in this work can be divided mainly into three parts.

- Catalyst Preparation System: The system is used for catalyst preparation including support preparation and incipient-to-wetness impregnation steps.
- Catalytic Reaction System: The system consists of a feed section including mass flow controllers, HPLC pump for water feed and a mixing zone; a reaction section composed of a continuous flow fixed-bed microreactor in a temperature controlled furnace.

- Product Analysis System: The analysis of the reactant and product streams is made using a gas chromatograph which is connected on-line to the microreactor flow system.

3.2.1. Catalyst Preparation Systems

The system used for catalyst preparation by incipient-to-wetness impregnation technique is presented in Figure 3.1. The system consists of a Retsch UR1 ultrasonic mixer, a Büchner flask containing catalyst support, a KNF Neuberger vacuum pump, a Masterflex computerized-drive peristaltic pump used for contacting the precursor solution to be impregnated with the support material, a beaker containing the precursor solution.

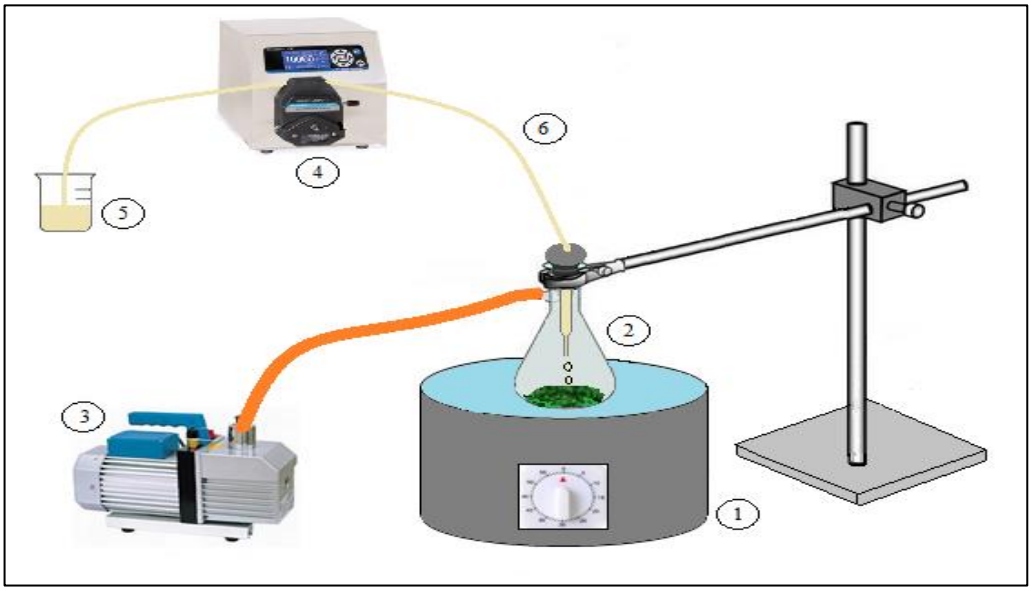

Figure 3.1. Schematic diagram of the impregnation system:
1. Ultrasonic mixer, 2. Büchner flask, 3. Vacuum pump, 4. Peristaltic pump, 5. Beaker, 6. Silicone tubing (Başar, 2016).

The system used for catalyst preparation by homogeneous deposition precipitation method is presented in Figure 3.2. It includes a Julabo ED-13 water bath, a beaker containing support material, a Heidolph RZR 2021 impeller and a Mettler Toledo FE20 pH-meter.

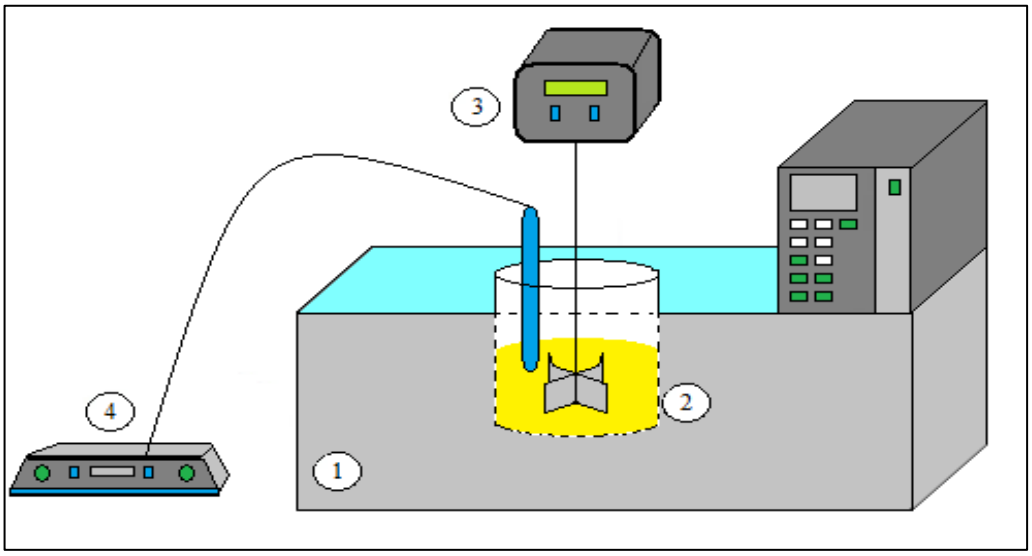

Figure 3.2. Schematic diagram of the deposition precipitation system:
1. Water bath, 2. Beaker, 3. Impeller, 4. pH-meter (Başar, 2016).

3.2.2. Catalytic Reaction System

The catalytic reaction system used in this study for WGS reaction was designed and constructed in the Catalysis and Reaction Engineering Laboratory of Chemical Engineering Department, Boğaziçi University. The system presented in Figure 3.3 consists of three sections: feed, reaction and product analysis.

The feed section consisted of the Brooks Instrument 0254 series mass flow controllers (MFCs) to control flow of the inlet gases and an Agilent Technologies 1200 series HPLC pump for water feed, 1/4'', 1/8'' and 1/16'' stainless steel tubes, valves and fittings for feeding liquid water and gases which are carbon monoxide, carbon dioxide, hydrogen, methane and argon. The reactant gases were supplied by pressurized cylinders at the pressure of 2.5 bar and the flow rate of gases were controlled by MFCs. On-off valves placed at exit of MFCs were used to protect them from possible back-pressure. Each gas was fed from an independent line in order to determine the flow of individual species.

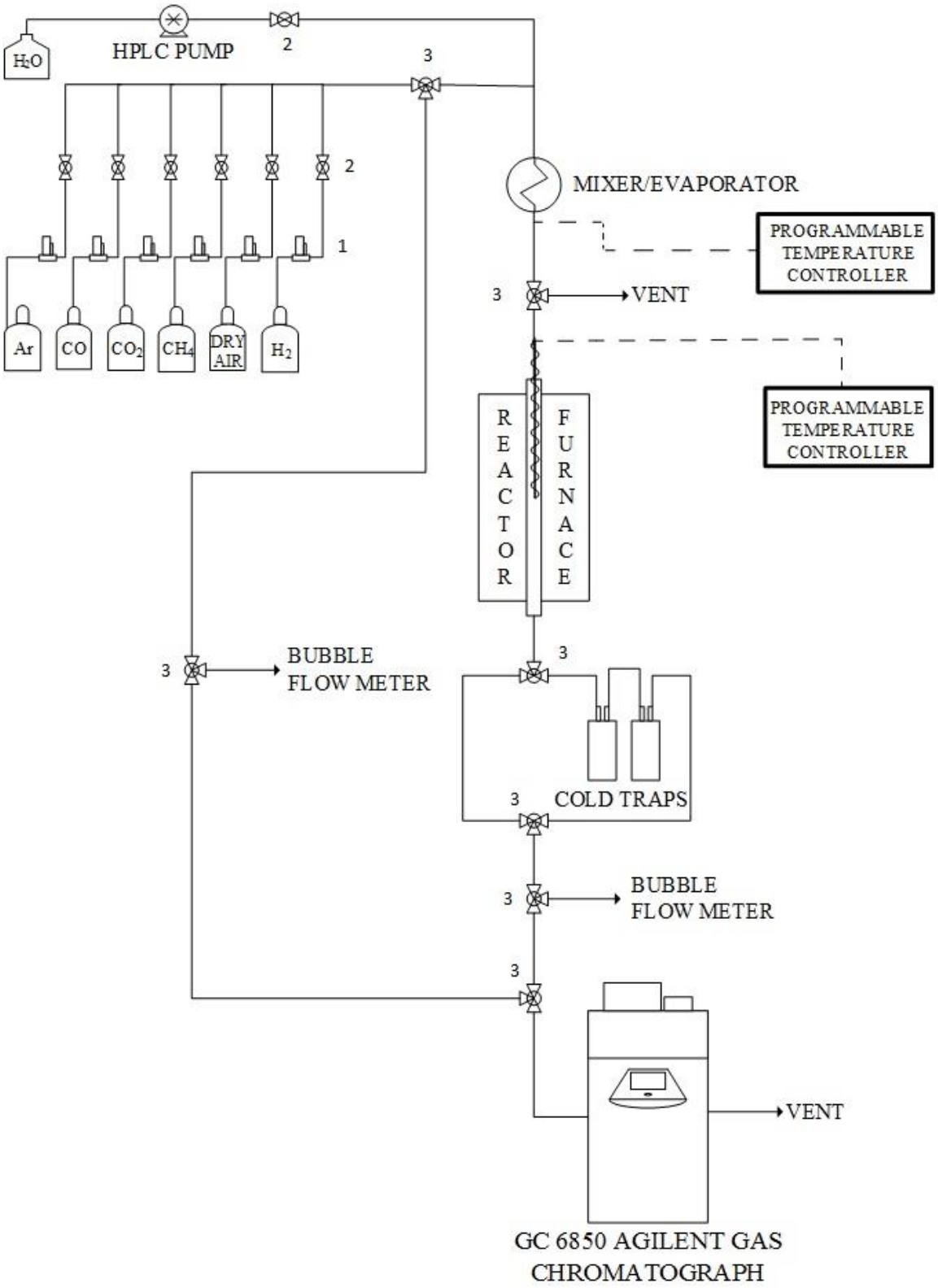

Figure 3.3. Schematic diagram of the microreactor flow system:

1. Mass flow controller, 2. On-off valve, 3. Three-way valve (Demirhan, 2015).

The liquid water was fed to the reaction system using HPLC pump. The 1/16" stainless steel (SS) tubing were kept about at 140 °C using a 104 W Cole-Parmer heating tape to enable complete vaporization of water before mixing zone. The temperature level of the mixer/evaporator line was controlled by a Eurotherm 3216 PID temperature controller connected to a K-type fiberglass coated thermocouple. Ceramic wool isolations were applied through the mixing line in order to prevent heat loss. In the mixing zone, all reactants including water vapor and gases were mixed prior to reaction.

The reaction section was composed of 50 cm x 20 cm x 20 cm furnace, a 71 cm long 1/4'' OD SS fixed bed microreactor, a Shimaden FP23 programmable temperature controller and a K-type sheathed thermocouple. A down-flow microreactor was placed inside the furnace. The catalyst bed was fixed at the center of the reactor using silane treated glass wool. K-type sheathed thermocouple, connected to the temperature controller, was placed inside furnace as shown in Figure 3.4. Ceramic wool insulations were placed in top and bottom ends of the reactor furnace to prevent heat loss. At the end of the reactor, a cold trap consisting of two condensers placed in an ice-water bed provided to remove water vapor from products since water vapor damages to gas chromatograph (GC) columns.

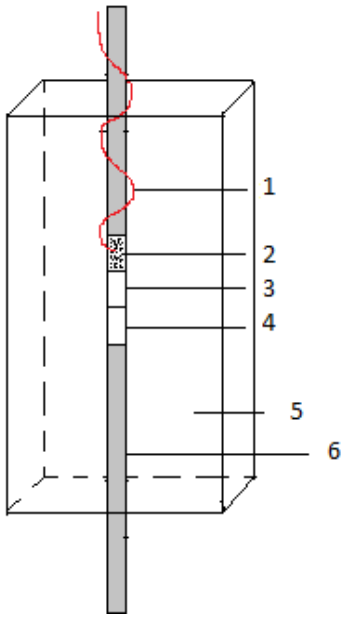

Figure 3.4. Schematic diagram of the reactor and oven system: 1. Thermocouple, 2. Catalyst + α-Al_2O_3, 3. α-Al_2O_3, 4. Glass wool, 5. Oven, 6. 1/4" reactor.

3.2.3. Product Analysis System

An Agilent Technologies 6850 gas chromatograph equipped with Hayesep D column, and a thermal conductivity detector (TCD) were used for analysis of feed and dry product compositions. Analysis conditions are given below in Table 3.4.

The GC was calibrated prior to the experiments to obtain the calibration curve so, known volumes of gases were injected to GC and peak areas were measured corresponding volumes of gases under the conditions given in Table 3.4. Volume percent versus peak area curves were plotted for each gas and calibration factors were determined by linear regression.

Table 3.4. Gas analysis conditions for WGS analysis system.

GC Specifications	**Agilent Technologies 6850**
Detector type	TCD
Column temperature, °C	40
Inlet temperature, °C	100
Detector temperature, °C	150
Carrier gas	Argon
Carrier gas flow rate, ml/min	15
Column packing material	Hayesep D
Column tubing material	Stainless steel
Column length & ID	3m x 3 mm
Sample loop	1 ml

3.3. Catalysis Preparation and Pretreatment

In this thesis, 1Pt-0.5Re-1V/CeO_2 catalyst was prepared which gave the highest performance in WGS tests conducted by Kesim, 2017. The catalyst was diluted with 250-354 μm (45-60 mesh) particle size α-Al_2O_3.

Ceria support was prepared using cerium (III) nitrate hexahydrate precursor, by homogeneous precipitation method with sodium carbonate being the precipitation agent. The sodium carbonate and cerium precursor was dissolved in water, separately. The Na_2CO_3 solution was slowly added to the cerium precursor containing solution, which was kept at 60 °C and stirred continuously in a water bath given in Figure 3.2, until the pH of the solution was adjusted to 8. The obtained suspension was then left for an hour in a water bath at 60 °C under controlled temperature. A stirred mixture was then filtered under vacuum by using Watman filter paper and washed with deionized water (DI) several times, and then dried overnight at 110 °C and calcined in muffle furnace at 400 °C for 4 hours (Çağlayan, 2011).

The trimetallic Pt-Re-V/CeO_2 catalyst (1wt.%Pt-0.5wt.%Re-1wt.%V) was prepared by a sequential route in which V precursor, Re precursor and Pt precursor solutions were added by the impregnation method in the system described in Figure 3.1.

First of all, V addition to CeO_2 support was conducted via incipient to wetness impregnation technique by using aqueous solution of ammonium meta-vanadate and oxalic acid dehydrate with 1:1.5 molar ratio. CeO_2 support was put in a Büchner flask and mixed in an ultrasonic mixer for 25 minutes under vacuum. The precursor solution of ammonium meta-vanadate and oxalic acid was impregnated on the support using a peristaltic pump at a rate of 0.5 ml/min. The resulting slurry was mixed ultrasonically for 1.5 h under vacuum and then dried overnight at 110 °C. The next morning, the slurry was for 2 h calcined at 400 °C in a muffle furnace.

Re-V/CeO_2 catalyst was prepared by the incipient-to-wetness impregnation technique by using aqueous solution of ammonium perrhenate. The aqueous solution was prepared by dissolving calculated amount of the precursor salt in definite amount of de-ionized water. Obtained V-impregnated CeO_2 support was placed in a Büchner flask and kept under vacuum and ultrasonic mixing for 25 minutes. The precursor solution was then impregnated on the support by using a peristaltic pump at a rate of 0.5 ml/min. The resulting thick slurry formed was left under vacuum and mixed ultrasonically for 1.5 h, then dried overnight at 110 °C and later on calcined at 400 °C for 2 h in a muffle furnace.

Finally, Pt addition to V and Re impregnated CeO_2 support was conducted via incipient to wetness impregnation technique by using aqueous solution of tetraammineplatinum (II) nitrate. The V and Re impregrated CeO_2 support was put in a Büchner flask and mixed in an ultrasonic mixer for 25 minutes under vacuum. The precursor solution was impregnated on the support using a peristaltic pump at a rate of 0.5 ml/min. The resulting slurry was mixed ultrasonically for 1.5 h under vacuum and then dried overnight at 110 °C. The next morning, the slurry was for 4 h calcined at 400 °C in a muffle furnace.

Prior to the reaction tests, the catalyst sample was placed into the constant temperature zone of the microreactor as shown in Figure 3.4. Pt-Re-V/CeO_2 catalyst sample was heated from room temperature to the reduction temperature of 375 °C at a rate of 8.75 °C/min under flow of 15% H_2/balance Ar mixture and then reduced for 2 hours at 375 °C.

3.4. WGS Reaction Tests

3.4.1. Blank Tests

Blank tests were conducted to ensure that the material of construction, glass-wool and α-alumina have no catalytic activity.

3.4.2. WGS Performance Tests

The WGS performance tests over 1Pt-0.5Re-1V/CeO_2 catalyst were carried out by Kesim at 300, 350 and 400 °C for two realistic feed compositions given in Table 3.5. The experiments were performed using 75 mg freshly reduced catalyst with 120,000 ml $gcat^{-1}h^{-1}$ GHSV for 6 hours TOS (Kesim, 2017).

Table 3.5. Realistic feed compositions used in performance study.

Feed	S/C	CO%	H_2O%	H_2%	CO_2%	Ar%
Realistic #1	6.7	4.9	32.7	30	10.4	22
Realistic #2	16.2	2.1	34.1	23.7	12.3	27.8

3.4.3. WGS Kinetic Tests

Kinetic tests in WGS reaction were performed to determine the power law type of rate expression of 1Pt-0.5Re-1V/CeO_2 catalyst as a function of temperature and partial pressures of CO, H_2O, H_2, CO_2 and CH_4. In the design of the experimental sets for kinetic study, a base experiment was selected in which CO, H_2O, H_2, CO_2 and CH_4 percentages were 2, 45, 15, 10 and 7%, respectively. The kinetic tests have been carried out at least for 3 different partial pressures of each species (i.e. carbon monoxide, steam, hydrogen, carbon dioxide, methane) for two different W/F values as shown given in Table 3.6. The base experiment was repeated and conducted also at 325 and 300 °C for activation energy calculations. With the intention of keeping conversions at low values, small amounts of catalyst (10 mg) were diluted with inert α-Al_2O_3 were put into the reactor such that the total bed weighed 100 mg. All WGS kinetic experiments were conducted in the reactor of the system shown in Figure 3.3. After reduction ended, the catalyst bed was brought to reaction temperature 350 °C under inert flow. Ar gas trapped in the reactor while the reactants with specified compositions were bypassed for 1.5 hour in order to obtain steady state gas composition. The reaction started with the first contact between reactant gases and catalyst bed. Product analyses were done at 15 and 30 minutes, 1, 2 and 4 hours. Feed analyses were done at the end of product analyses.

Table 3.6. List of kinetic experiments performed over 1Pt-0.5Re-1V/CeO_2 catalyst.

Run #		Total flow rate ($ml\ min^{-1}$)	Percentage in feed stream						
			CO	H_2O	H_2	CO_2	CH_4	Ar	H_2O/CO
1	a	250	1	45	15	10	7	22	45
	b	200	1	45	15	10	7	22	45
2	a	250	2	45	15	10	7	21	22.5
	b	200	2	45	15	10	7	21	22.5
3	a	250	3	45	15	10	7	20	15
	b	200	3	45	15	10	7	20	15
4	a	250	2	60	15	10	7	6	30
	b	200	2	60	15	10	7	6	30
5	a	250	2	50	15	10	7	16	25
	b	200	2	50	15	10	7	16	25
6	a	250	2	30	15	10	7	36	15
	b	200	2	30	15	10	7	36	15
7	a	250	2	45	15	11	7	20	22.5
	b	200	2	45	15	11	7	20	22.5
8	a	250	2	45	15	9	7	22	22.5
	b	200	2	45	15	9	7	22	22.5
9	a	250	2	45	15	8	7	23	22.5
	b	200	2	45	15	8	7	23	22.5
10	a	250	2	45	18	10	7	18	22.5
	b	200	2	45	18	10	7	18	22.5
11	a	250	2	45	16	10	7	20	22.5
	b	200	2	45	16	10	7	20	22.5
12	a	250	2	45	12	10	7	24	22.5
	b	200	2	45	12	10	7	24	22.5
13	a	250	2	45	15	10	9	19	22.5
	b	200	2	45	15	10	9	19	22.5
14	a	250	2	45	15	10	8	20	22.5
	b	200	2	45	15	10	8	20	22.5
15	a	250	2	45	15	10	6	22	22.5
	b	200	2	45	15	10	6	22	22.5
16	a	250	2	45	15	10	5	23	22.5
	b	200	2	45	15	10	5	23	22.5
17	a	250	2	45	15	10	0	28	22.5
	b	200	2	45	15	10	0	28	22.5

A power law fit can adequately describe the activity of the WGS reaction over broad ranges of temperature and composition for the noble-metal catalyst (Dijk *et al*., 2010). The general form of the power law rate equation for kinetic test conditions given above is:

$$-r_{CO} = kP_{CO}^{\alpha}P_{H_2O}^{\beta}P_{H_2}^{\delta}P_{CO_2}^{\gamma}P_{CH_4}^{\varepsilon}(1-\beta') \tag{3.1}$$

where the term β' represents the factor of reversible reaction.

$$(1-\beta') = \left(1 - \frac{1}{K_{eq}}\frac{P_{H_2}P_{CO_2}}{P_{CO}P_{H_2O}}\right) \tag{3.2}$$

The higher β' value causes an increase in the reverse reaction rate. In order to use the method of initial rates, the β' value should be kept as low as possible.

4. RESULTS AND DISCUSSION

In the foreseeable future, the use of technologies enabling non-intermittent energy production through highly efficient ways/routes from renewable resources will be well proliferated. The continuous renewable energy production, that can satisfy a significant fraction of the base load on a grid, will also help the extensive use of flow limited renewable energy production routes, like solar and wind. One of non-intermittent energy production ways is the use of small scale on site electricity production via combined fuel processor-PEM fuel cell (FP-PEMFC) systems operating with bio-methane as the hydrocarbon feed.

In general, FPs convert a hydrocarbon, *having well-established distribution network and/or easy-to store*, like methane, propane, or their mixture, like LPG, into hydrogen rich reformate feed for the FCs. In FPs, 3 catalytic reactions occur in series: reforming of hydrocarbons; water-gas shift (WGS); and preferential carbon monoxide oxidation (PROX). Specifically for FP-PEMFC applications, the hydrogen rich FP product stream must be PEM-grade, ie. CO content is lower than 100 ppm; and oxidative steam reforming (OSR), which can reach high hydrocarbon conversion level at temperatures lower than those used in steam reforming (SR), is usually the preferred reforming reaction.

The aim of the current study is to obtain a reliable power-law type kinetic expression valid for real feed conditions for WGS reaction over 1Pt-0.5Re-1V/CeO_2 catalyst to be used in designing the WGS unit of a small scale FP. In determination of the feed conditions used in the kinetic tests, an average OSR product distribution, which was experimentally obtained in our previous study (Başar, 2016), was used as the reference basis. Unlike previous kinetic studies, the current study additionally assessed the effect of methane presence in the feed on WGS kinetics. The results of this study are considered as an important element of the overall design, optimization and control of a demo-scale FP, which will have capacity to produce hydrogen for a 1 kW PEMFC, is being currently developed by our group.

The results are presented in three sections. First section outlines the results of WGS performance tests previously performed by our group (Kesim, 2017). In the second section, the results of the preliminary kinetic tests conducted to determine the temperature, S/C feed ratio and W/F ranges ensuring mass transfer free regime are presented. The final section includes the results of the kinetic studies conducted, and the power-law type kinetic expression proposed for WGS over the Pt-Re-V catalyst.

4.1. Performance Tests of WGS over Pt-Re-V/CeO_2 Catalysts

The performance of the Pt-Re-V/CeO_2 series catalysts under realistic feed conditions were studied previously by our group (Kesim, 2017); the test results revealed that 1Pt-0.5Re-1V/CeO_2 has the highest performance**.** The performance characteristics of the catalyst is summarized in this section.

In performance tests, temperature and steam-to-carbon ratio (S/C) were used as experimental parameters. The tests were conducted at three different temperature levels, 300, 350 and 400 °C for realistic feed 1# having S/C 6.7 and realistic feed 2# having S/C 16.2, as given in Table 3.5. All performance tests were performed under atmospheric pressure over 75 mg freshly reduced catalyst with fixed GHSV as 120,000 ml $gcat^{-1}$ h^{-1}. Conversion values at the end of 2 h TOS (time-on-stream) were used as the activity measure. The CO conversion was calculated according to Equation 4.1.

$$\text{CO conversion (\%)} = \left(\frac{f_{CO,in} - f_{CO,out}}{f_{CO,in}}\right) \times 100 \qquad (4.1)$$

where f is the molar flow rate of CO. Activity loss, which is a measure of stability of the catalyst, was calculated as the percentage loss in activity at the end of 6 h TOS on the basis of activity at the end of 0.5 h TOS, according to Equation 4.2.

$$\text{Activity loss (\%)} = \left(\frac{[\text{CO conversion}]_{0.5h} - [\text{CO conversion}]_{6h}}{[\text{CO conversion}]_{0.5h}}\right) \times 100 \qquad (4.2)$$

The activity losses calculated for various reaction temperatures under the flow of both realistic feeds over 1Pt-0.5Re-1V/CeO_2 are presented in Figures 4.1 and 4.2. The activity losses in 6 h TOS tests were calculated as 7.4%, 3.4% and 22.7% for the realistic feed #1 at temperatures 350 °C, 400 °C and 300 °C, respectively. Higher activity losses were observed at 300 °C for both feed conditions (Kesim, 2017).

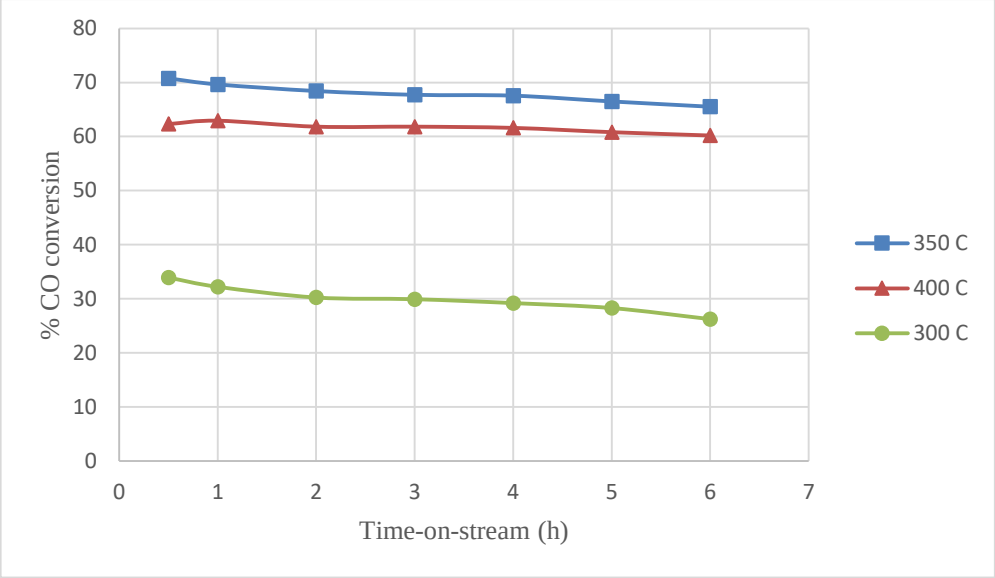

Figure 4.1. Time-on-stream activity for realistic feed #1 for different temperatures.

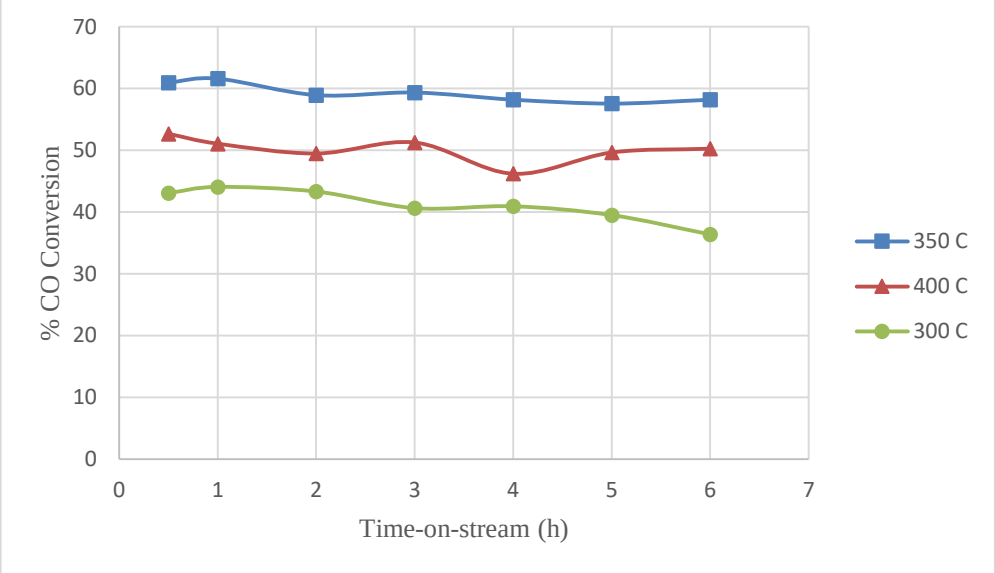

Figure 4.2. Time-on-stream activity for realistic feed #2 for different temperatures.

The effect of temperature on catalytic activity was studied for 300-400 °C temperature range; the CO conversion values (*for 2 h TOS*) are presented in Figure 4.3 for S/C ratio of 6.7, and in Figure 4.4 for S/C ratio of 16.2. The equilibrium CO conversions were calculated by using HSC-Chemistry Software.

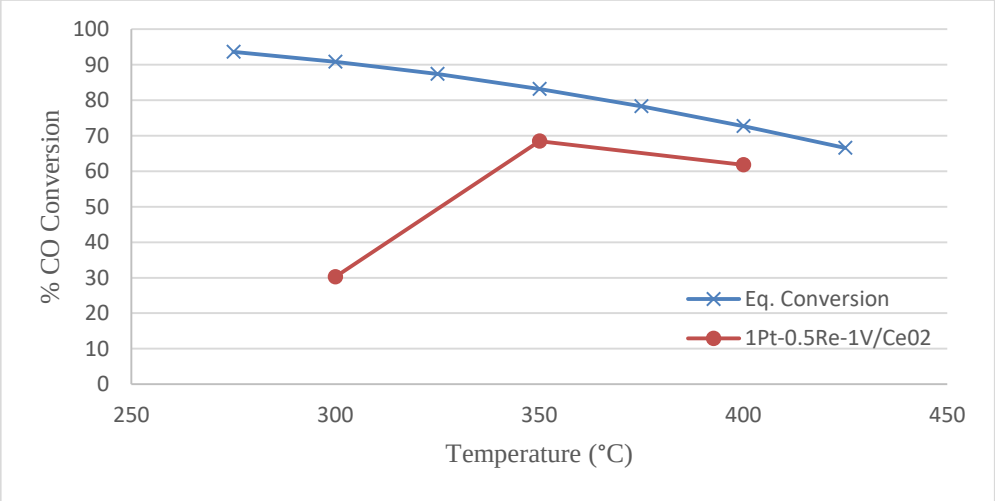

Figure 4.3. Temperature dependency of catalytic activity of 1Pt-0.5Re-1V/CeO_2 for realistic feed #1.

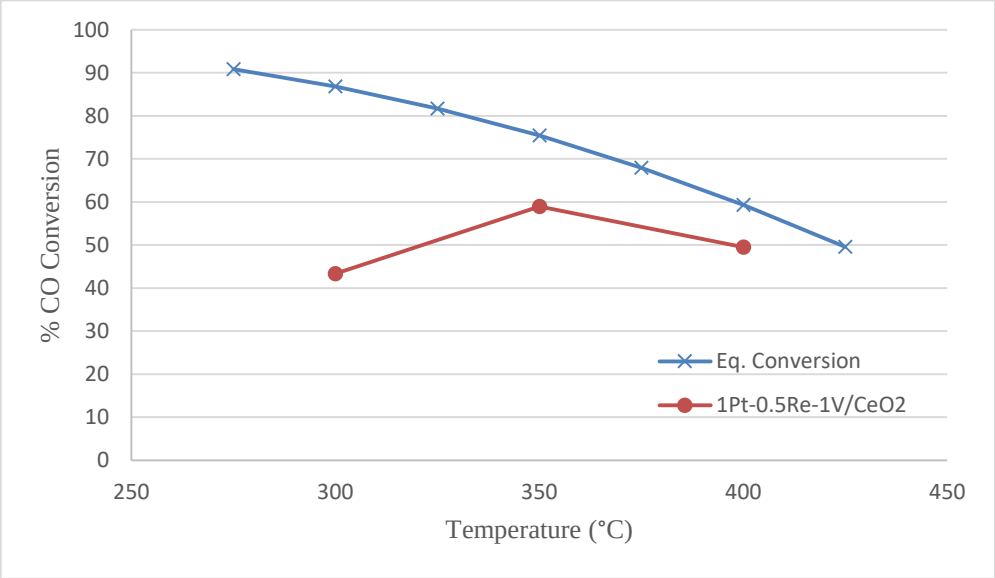

Figure 4.4. Temperature dependency of catalytic activity of 1Pt-0.5Re-1V/CeO_2 for realistic feed #2.

The results show that WGS activity increased with increasing reaction temperature for both feed conditions until 350 °C. However, further increase in temperature led to significant activity decrease. 1Pt-0.5Re-1V/CeO_2 showed its highest activity for realistic feed #1 at 350 °C reaching 68.42% conversion as opposed to 83.18% equilibrium conversion limit. Under realistic feed #2 conditions, for which thermodynamic equilibrium conversion was calculated as 75.42%, 58.92% conversion was obtained. It should be noted that increasing H_2O/CO feed ratio from 6.7 to 16.2 resulted in higher CO conversion at 300 °C, whereas lower conversions at both 350 °C and 400 °C (Kesim, 2017).

As it is desired to maximize hydrogen production, selectivity is always considered as an important performance measure of a WGS catalyst. Unwanted methane formation, which consumes valuable hydrogen, should be avoided in WGS reactions. 1Pt-0.5Re-1V/CeO_2 showed no methanation activity for all experimental conditions, indicating that the Pt-Re-V systems suppresses secondary methanation activity (Kesim, 2017). The results revealed that 1Pt-0.5Re-1V/CeO_2 is an appropriate catalyst to be used in a fuel processor for WGS reaction owing to its high activity, stability and selectivity.

4.2. Kinetic Preliminary Tests of WGS over Pt-Re-V/CeO_2 Catalyst

The aim of preliminary kinetic tests is to find the optimum experimental parameters' ranges ensuring the kinetic tests are conducted within kinetically controlled and mass transfer limitation free region; thus, CO conversion should be kept minimal as much as possible under reasonable (*ie. as close as possible to real*) reaction conditions.

For the kinetic experiments, the optimum reaction temperature was selected as 350 °C, which ensures the highest catalyst activity (see Section 4.1). The amount of catalyst used was reduced from 75 mg to 10 mg in order to decrease CO conversion and achieve kinetically controlled region. In each test, the catalyst was diluted with α-Al_2O_3 such as to keep total bed weight fixed at 100 mg. Blank tests were performed to ensure that the reactor, glass wool and α-Al_2O_3 had no catalytic activity. In addition, unlike performance tests, the total flow rate was increased from 150 ml min^{-1} to 200 ml min^{-1}. For obtaining initial rates with high confidence, the trendline in conversion versus residence time (W/F_{CO} ratio) should show a linear relationship. In the preliminary experiments, for two different

residence time values, GHSV was taken as $1.2*10^6$ and $1.5*10^6$ ml $gcat^{-1}$ h^{-1} corresponding to 200 ml min^{-1} and 250 ml min^{-1} flow rates, respectively, for fixed, 10 mg, catalyst amount.

Considering the fact that WGS reactor in a FP uses OSR product as its feed; real WGS feed composition ranges should be defined based on experimentally measured propane OSR product compositions obtained over the OSR catalyst used by our group, Pt-Ni/Al_2O_3, for various reaction conditions (Başar, 2016; see Table 4.1). In kinetic tests, the real WGS feed composition is defined as the average composition of the OSR products obtained in the OSR tests conducted at 400 and 450 °C for S/C feed ratios of 3 and 6.

Table 4.1. Propane OSR product compositions obtained in the OSR tests conducted at 400 and 450 °C for S/C feed ratios of 3 and 6 (Başar, 2016).

		Wet Based Product Concentration (%)							
T_{OSR} (^{0}C)	**S/C**	H_2	CO	CH_4	CO_2	C_3H_8	O_2	H_2O	He
400	3.00	13.4	0.32	9.5	11.0	0.032	0.004	41.9	23.9
400	6.00	13.5	0.35	5.4	7.7	0.045	0.004	58.2	14.7
450	3.00	18.5	1.09	8.6	12.0	0.031	0.005	36.5	23.2
450	6.00	16.1	0.66	5.0	8.1	0.016	0.004	55.3	14.7

Although the average OSR product composition is the feed used in Run 1 of the kinetic tests (given in Table 3.6); the reference basis feed composition was selected as used in Run 2; since for the feed used in Run 1, the (β') value in Equation 4.4, which is the measure showing the closeness to equilibrium, was bigger than 0.1 indicating the reaction was carried out close to equilibrium region rather than initial rate region. For Run 1 conditions, there is slightly higher inhibitory effect, which is undesired for kinetic tests, coming from H_2 and CO_2 on forward reaction compared to that for Run 2.

In preliminary tests, Run 2a-2b experiments (Table 3.6) were conducted and duplicated at 350 °C using 10 mg catalyst weight for both flow rates, ie. 200 ml min^{-1} and 250 ml min^{-1}. The results are presented in Figure 4.5; the plots had high R^2 values, which showed that the experiments were in kinetically controlled region.

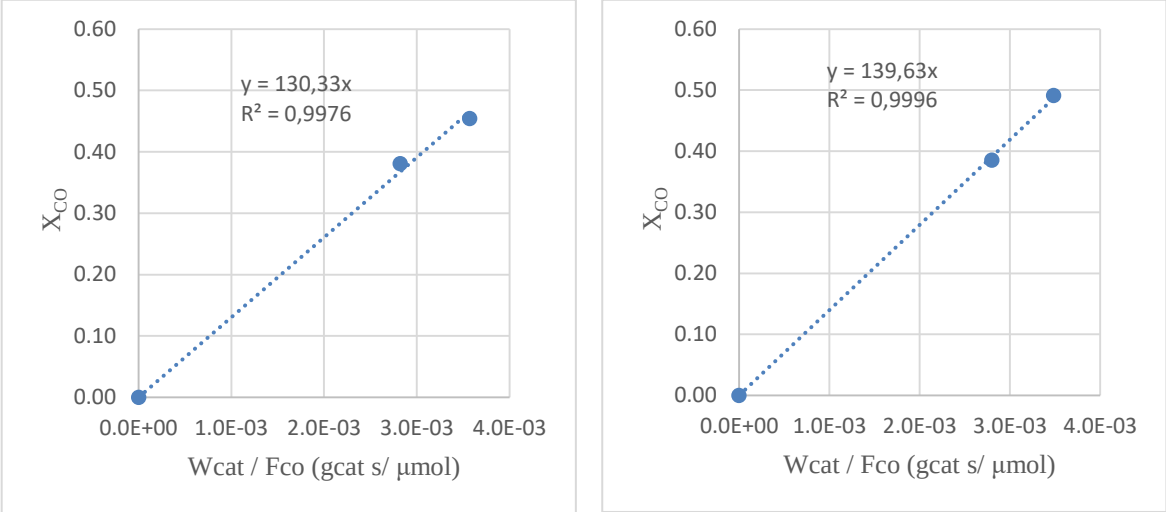

Figure 4.5. CO conversion levels of Run 2a-2b repeated in duplicate.

4.3. Kinetic Tests of WGS over Pt-Re-V/CeO_2 Catalyst

The kinetic tests were performed at 350 °C by changing the partial pressures of reactants according to feed conditions given in Table 3.6. Argon was used as inert to balance total flow rate. CO concentrations were changed between 1% and 3% resulting H_2O/CO feed ratios ranging from 15 to 45. The power law type rate expression was aimed to be obtained in terms of CO, H_2O, H_2, CO_2 and CH_4 concentrations. Initial rate for each feed condition was obtained by varying W_{cat}/F_{CO} ratio through changing flow rate while keeping all other reaction parameters constant. The initial reaction rate ($-r_{CO}$) was calculated according to Equation 4.3.

$$-r_{CO} = \frac{dX_{CO}}{d(W_{cat}/F_{CO})} \tag{4.3}$$

where $-r_{CO}$ is the reaction rate in µmol g^{-1} s^{-1}, X_{CO} is carbon monoxide conversion, W_{cat} is catalyst weight in g and F_{CO} is carbon monoxide flow rate in µmol s^{-1}.

The reaction rates given in Table 4.2 were calculated from slopes of the conversion versus residence time plots given in Appendix A. The reaction orders of the power-law type rate expression presented in Equation 4.4 were calculated by using the initial rate data given in Table 4.2.

$$-r_{CO} = [k_0 e^{(-\frac{E_A}{RT})}] P_{CO}^{\alpha} P_{H_2O}^{\beta} P_{H_2}^{\delta} P_{CO_2}^{\gamma} P_{CH_4}^{\varepsilon} (1 - \beta') \quad (4.4)$$

In Equation 4.4, α, β, δ, γ and ε are the reaction orders of each component, k_0 is the pre-exponential factor, E_A is the activation energy (kJ mol^{-1}), R is the universal gas constant (kJ mol^{-1} K^{-1}), T is the temperature (K) and P is the partial pressures (kPa) of each component. The equilibrium nature of the reaction is reflected by the parameter β', which is expressed as:

$$\beta' = \frac{1}{K_{eq}} \frac{P_{H_2} P_{CO_2}}{P_{CO} P_{H_2O}} \quad (4.5)$$

Equilibrium constant was calculated as 20.45 at 350 °C using Equation 4.6.

$$K_{eq} = \exp\left(\frac{4577.8}{T} - 4.33\right) \quad (4.6)$$

In order to calculate reaction orders, natural logarithm of Equation 4.4 was taken and linear regression was applied.

$$\ln(-r_{CO}) = lnk + \alpha \ln(P_{CO}) + \beta \ln(P_{H_2O}) + \delta \ln(P_{H_2}) + \gamma \ln(P_{CO_2}) + \varepsilon ln(P_{CH_4}) \quad (4.7)$$

17 pairs of kinetic experiments were conducted for different partial pressures of reactants and residence time. Initial reaction rates were obtained from the slopes of "CO conversion versus residence time" plots. The reported WGS reaction orders in the literature were estimated for methane free feeds. In the current study, besides the WGS reactants and products, the contribution coming from methane presence on rate was also analyzed; methane concentration in the feed was kept constant in 12 pairs of kinetic experiments, whereas it was changed for the rest of the tests. The initial reaction rate values calculated along with associated goodness-of-fit values, R^2, as a measure of linear relation between rate and W/F, are given in Table 4.2.

Table 4.2. Feed stream conditions and corresponding initial rates of WGS over 1Pt-0.5Re-1V/CeO_2 at 350 °C.

	Partial Pressures (kPa)							
	CO	**H_2O**	**H_2**	**CO_2**	**CH_4**	**Reaction Rate (μmol/ g s)**	**(1-β')**	**R^2**
1a-1b	1.01	45.60	15.20	10.13	7.09	73.50	0.837	0.9948
2a-2b	2.03	45.60	15.20	10.13	7.09	134.90	0.919	0.9922
3a-3b	3.04	45.60	15.20	10.13	7.09	209.33	0.946	0.9920
4a-4b	2.03	60.80	15.20	10.13	7.09	163.30	0.939	0.9937
5a-5b	2.03	50.66	15.20	10.13	7.09	153.34	0.927	0.9968
6a-6b	2.03	30.40	15.20	10.13	7.09	122.60	0.878	0.9899
7a-7b	2.03	45.60	15.20	11.15	7.09	128.13	0.910	0.9715
8a-8b	2.03	45.60	15.20	9.12	7.09	137.86	0.927	0.9897
9a-9b	2.03	45.60	15.20	8.11	7.09	154.84	0.935	0.9849
10a-10b	2.03	45.60	18.24	10.13	7.09	129.72	0.902	0.9991
11a-11b	2.03	45.60	16.21	10.13	7.09	130.02	0.913	0.9625
12a-12b	2.03	45.60	12.16	10.13	7.09	149.52	0.935	0.9888
13a-13b	2.03	45.60	15.20	10.13	9.12	135.92	0.919	0.9848
14a-14b	2.03	45.60	15.20	10.13	8.11	146.93	0.919	0.9972
15a-15b	2.03	45.60	15.20	10.13	6.08	137.27	0.919	0.9952
16a-16b	2.03	45.60	15.20	10.13	5.07	135.24	0.919	0.9818
17a-17b	2.03	45.60	15.20	10.13	0.00	133.19	0.919	0.9644

The β' value lower than 0.1 for a feed accepted as the measure that reverse-WGS has practically no effect on rate. All the β' values for the kinetic test runs were lower than 0.1, indicating desired kinetic test conditions far from equilibrium, with the exception of Run 1 and 6, for which β' values were slightly greater than 0.1. The initial rate values obtained from the 17 pairs of experiments were used to calculate reaction orders through non-linear multivariable optimization analysis performed in MATLAB™ environment; the calculated rate orders are presented in Table 4.3.

The proposed power law type rate expression shows a positive dependence on CO and H_2O. However, an increase in H_2 and CO_2 concentrations caused a decrease in the conversion levels (Table 4.3). The contribution of methane partial pressure to the reaction rate was found insignificant as there was no change in the predicted reaction orders of CO, steam, H_2 and CO_2 in the absence and presence of methane term in the rate expression. It should be also noted that in presence of methane term, the reaction order with respect to methane is 0.002; this very small order indicates practically no effect of methane presence in the feed stream on WGS rate.

Table 4.3. Reaction orders for WGS reaction over 1Pt-0.5Re-1V/CeO_2.

Number of experiment sets	**α**	**β**	**δ**	**γ**	**ε**
17	0.82	0.31	-0.29	-0.35	0.002
12	0.82	0.31	-0.29	-0.35	-

It should be noted that 5 pairs of experiments were conducted aiming to observe the methane effect on reaction rate and the results are given in Figure 4.6. The results clearly show methane presence has insignificant effect and confirmed very low order in the rate expression with respect to methane.

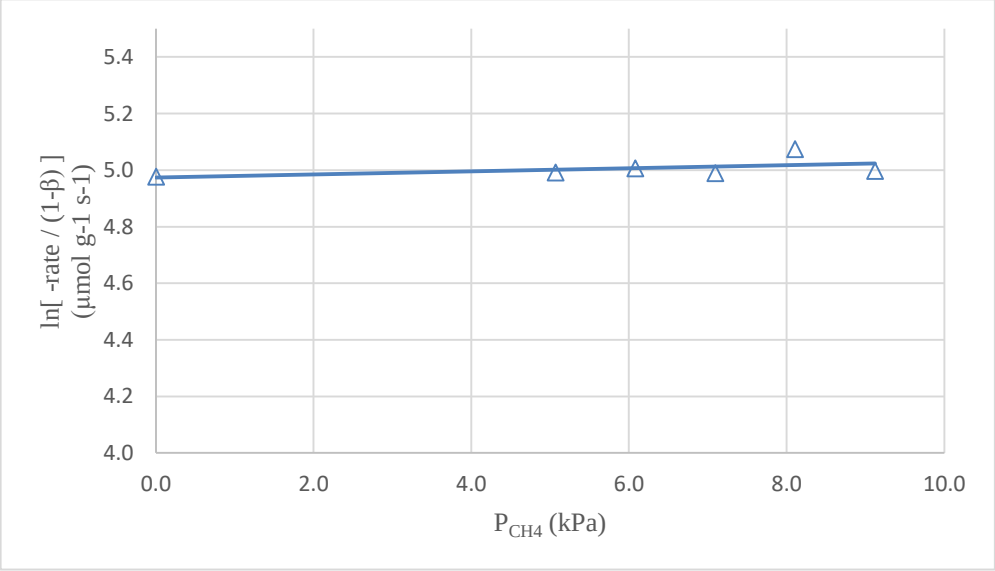

Figure 4.6. The effect of methane partial pressure on WGS reaction rates.

Most of the studies in the literature were carried out under different reaction conditions; therefore, a comparison of reaction orders calculated in the current study and the ones proposed in the literature is rather difficult. Additionally, as the current study was performed for real feed conditions; a healthy comparison is only possible when the inhibitory effect of H_2 and CO_2 on forward reaction is considered. Many kinetic studies reported over noble metal supported catalysts revealed almost zero-order depencency of reaction rate on CO (Ovesen *et al.*, 1992; Bunluesin *et al.*, 1998; Hilaire *et al.*, 2001; Radhakrishnan *et al.*, 2006; Phatak *et al.*, 2007; Azzam *et al.*, 2008). According to kinetic studies reported in the literature it can be inferred that at high CO concentrations, the reaction order with respect to CO is close to zero, whereas it becomes positive for lower CO concentrations since the surface coverage of adsorbed CO affects the reaction rate (Phatak *et al.*, 2007). Increase in the saturation of active metal sites with CO results in lower reaction orders. Additionally, surface coverage of CO decreases, and the observed reaction becomes first order with respect to CO in response to an increase in temperature (Jacobs *et al.*, 2003). As the WGS kinetics was determined at high temperature for low CO concentrations in the current study, the proposed reaction order with respect to CO, 0.82, is in agreement with those reported in the literature (Choi and Stenger, 2003; Koryabkina *et al.*, 2003; Kalamaras *et al.*, 2009).

Phatak *et al.* (2007) investigated the reaction order with respect to H_2O over Pt/Al_2O_3 and Pt/CeO_2, and found as 1.0 and 0.44, respectively. The difference in order could be explained through different reaction mechanisms occur on these catalysts. In addition, Bunluesin *et al.*, (1998) proposed that the metal component did not play a significant role for the reaction order with respect to water. In the current study, the reaction order with respect to H_2O was found 0.31, which is in agreement with the results of Hilaire *et al.* (2001), Koryabkina *et al* (2003) and Leppelt *et al.* (2006). The approximately half-order dependency for H_2O indicates that the reaction rates were partially limited by reoxidation of ceria.

The negative dependence on CO_2 and H_2 could be explained by the inhibition of the forward WGS reaction according to Le Chatelier's principle. The negative reaction order, (-0.29), with respect to H_2 and (-0.35) with respect to CO_2 indicates the effect of reverse WGS on net rate especially when the concentration of the WGS products are high. The

reason of negative dependency for H_2 is uncertain. Hilaire *et al*. (2001) and Kalamaras *et al*. (2009) have proposed that the negative dependency with respect to H_2 could be originated from the competitive adsorption of H_2 with CO. However, Azzam *et al*. (2008) have disagreed with that explanation as they proposed CO adsorption was known to be much more facile than ‘‘H’’ on Pt. They suggested that hydrogen inhibited the WGS over Pt-based catalysts via suppressing the formation of OH groups on support. In the current study, the reaction order with respect to H_2 was found as (-0.29), which was small compared to the ones proposed in the literature. This can be considered reasonable under the light of the findings by Radhakrishnan *et al*. (2006) who mentioned that Re addition to Pt-based catalyst led to smaller negative orders for CO_2 and H_2.

The reported apparent reaction orders in the literature were usually estimated for a methane free feed, whereas the current study was carried at a methane concentration of 7%. In any case, the WGS kinetics was found practically independent from the concentration of CH_4 in the feed stream.

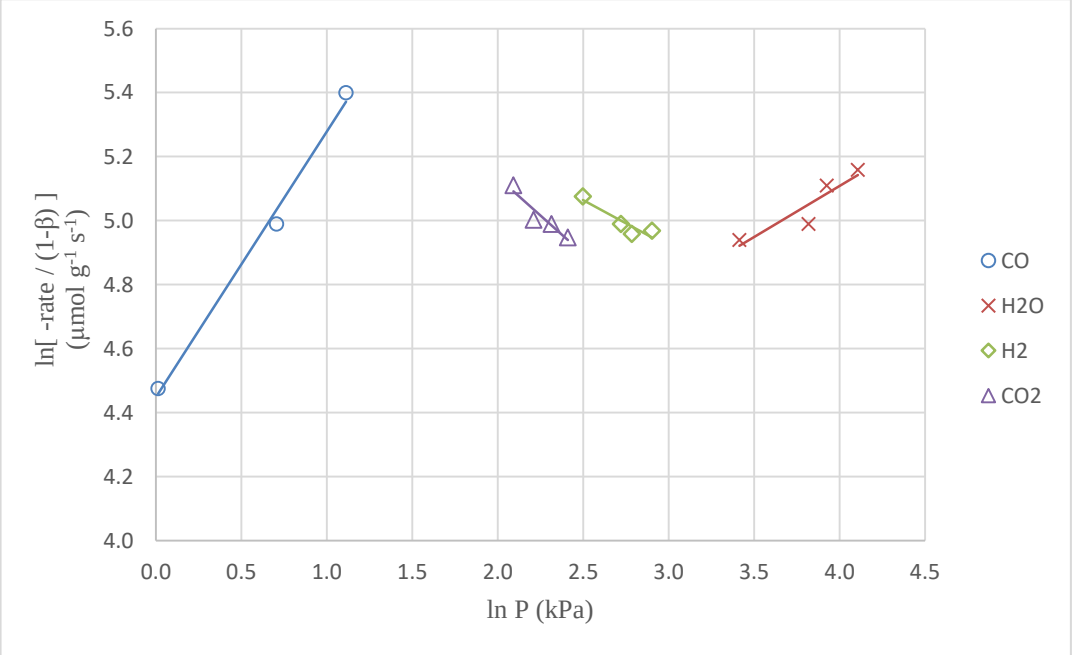

Figure 4.7. The effects of CO, H_2O, H_2, CO_2 partial pressures on WGS reaction rates.

Natural logarithm plots of [CO consumption rate / (1-β')] versus component partial pressures are presented in Figure 4.7. All the plots showed linear relationship, ensuring that the empirical power law type rate expression is appropriate for modeling the kinetics of WGS reaction. The reaction orders corresponding to each species could be also estimated by using the slope of straight lines of the natural log-log plots. Increase in CO_2 and H_2 concentrations caused a decrease in the conversion rate, which is confirmed by negative slopes of the [CO consumption rate / (1-β')] vs. partial pressures of those species.

As the performance tests conducted on 1Pt-0.5Re-1V/CeO_2 before revealed that its WGS activity decreased at temperatures higher than 350 °C (Kesim, 2017), the temperature range for determining apparent activation energy was selected as 300-350 °C; and accordingly, the base experiment (Run 2a-2b) was repeated at 300 and 325 °C. The apparent activation energy was calculated through utilizing the results in the linearized form of Arrhenius equation (Equation 4.8), and the estimated kinetic parameters were obtained by linear regression are represented in Table 4.4. The linearized form of Arrhenius equation for 300-350 °C temperature interval was plotted in Figure 4.8.

$$k = k_0 e^{(-\frac{E_A}{RT})} \tag{4.8}$$

Table 4.4. Kinetic parameters of WGS over 1Pt-0.5Re-1V/CeO_2.

Parameter	**Unit**	**Estimate**
k_0	μmol $gcat^{-1}$ s^{-1} $kPa^{-0.49}$	29209
E_A	kJ mol^{-1}	28.215

The activation energy was calculated as 28.21 kJ mol^{-1} in a temperature range of 300-350 ºC. The results were in agreement with the findings of Gökaliler *et al*. (2013) who reported activation energy of WGS as 28 kJ/mol over Au-Re/CeO_2 catalyst. On the other hand, as the inhibitory effects of H_2 and CO_2 have not been considered in most studies in the literature, *ie. the experiments were performed only for ideal feed*, a comparison between currently calculated E_A value with those reported in literature would not healthy; it should be noted that ignoring the inhibition could result in an apparent activation energy values lower than the actual one (Koryabkina *et al*., 2003).

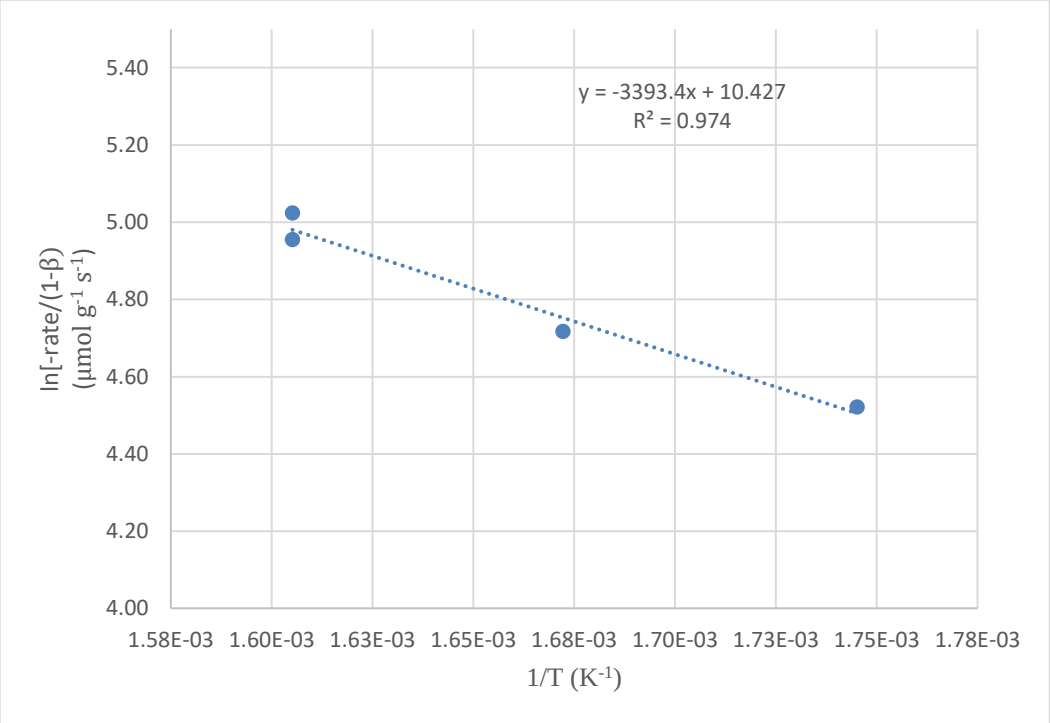

Figure 4.8. Arrhenius plot for WGS reaction over 1Pt-0.5Re-1V/CeO_2.

The power-law type rate expression of WGS reaction over 1Pt-0.5Re-1V/CeO_2 is presented in Equation 4.9.

$$-r_{CO} = [29209e^{(-\frac{28215}{8.314\times T})}]P_{CO}^{0.82}P_{H_2O}^{0.31}P_{H_2}^{-0.29}P_{CO_2}^{-0.35}P_{CH_4}^{0.002}(1-\beta') \quad (4.9)$$

In order to analyze the accuracy of the predicted reaction rates, the calculated and experimentally measured WGS (ie. CO consumption) rates were compared for the same reaction conditions. The corresponding plot in Figure 4.9 shows that the power-law type rate expression is reliable to predict overall CO conversion rates quantitatively within 6% error margin.

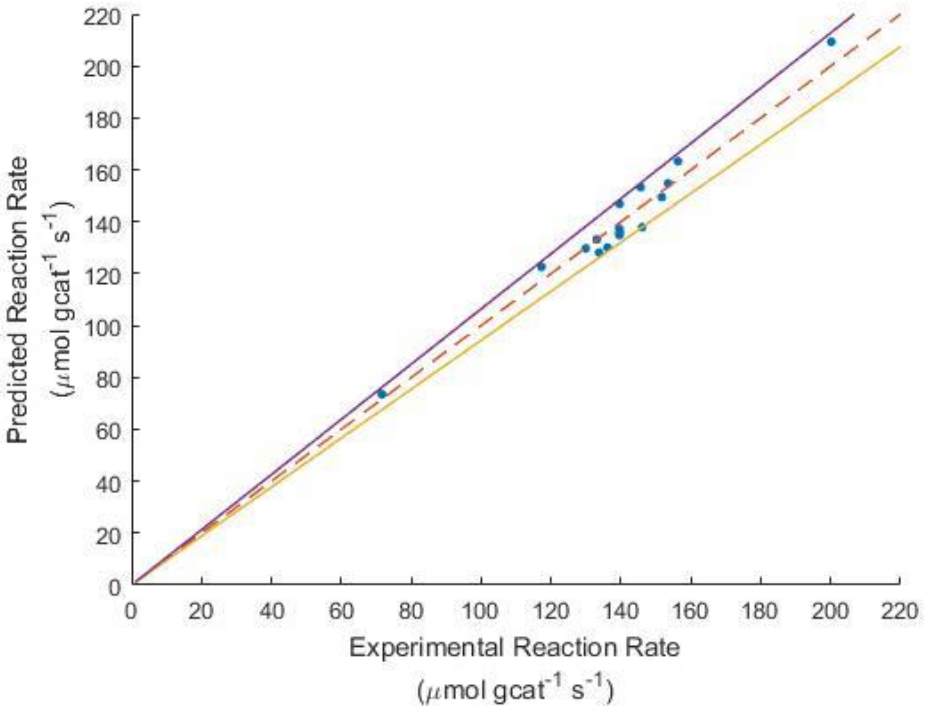

Figure 4.9. Experimental versus predicted CO consumption rates within $\pm$ 6% error.

5. CONCLUSIONS

5.1. Conclusions

In this study, a reliable power-law type kinetic expression valid for real feed conditions for WGS reaction over 1Pt-0.5Re-1V/CeO_2 catalyst was obtained to be used in designing the WGS unit of small-scale fuel processor. The kinetic experiments were carried out under fully real feed conditions, obtained from product concentrations of OSR, at 350 °C by changing the partial pressures of reactants according to feed conditions given in Table 3.6. Unlike previous kinetic studies, the current study additionally assessed the effect of methane presence in the feed on WGS kinetics.

In the preliminary kinetic tests, carbon monoxide conversion was kept minimal as much as possible under reasonable reaction conditions to ensure mass transfer limitation free intervals suitable for the kinetic tests. For the kinetic experiments, the optimum reaction temperature was selected as 350 °C, which ensures the highest catalyst activity. The amount of catalyst used was reduced from 75 mg to 10 mg in order to decrease CO conversion and achieve kinetically controlled region. Catalyst weight were diluted with a-Al_2O_3 to eliminate axial dispersion so that the total bed weight was fixed at 100 mg. In order to obtain different residence times, GHSV was taken as $1.2*10^6$ and $1.5*10^6$ ml $gcat^{-1}$ h^{-1} corresponding to 200 ml min^{-1} and 250 ml min^{-1} flow rates, respectively.

17 pairs of kinetic experiments were conducted for different partial pressures of reactants and residence time. Initial reaction rates were obtained from the slopes of CO conversion versus residence time plots. Methane partial pressure was kept constant in 12 pairs of kinetic experiments, whereas it was changed for the rest of the tests in order to see the contribution of methane partial pressure on the reaction rate, since the reported reaction orders in the literature were usually estimated for methane free feeds. The power-law kinetic model of WGS reaction over 1Pt-0.5Re-1V/CeO_2 catalyst was estimated by using the method of initial rates within ±6% error. The reaction orders for the proposed kinetic model were obtained as 0.82, 0.31, -0.29, -0.35 and 0.002 for carbon monoxide, steam, hydrogen, carbon dioxide and methane, respectively by non-linear regression analysis

performed in MATLAB^{TM}. The rate expressions were obtained with positive dependence on CO and H_2O. Negative reaction orders with respect to CO_2 and H_2O was obtained, which indicated the inhibitory effect of CO_2 and H_2O on the reaction rate. Since the reaction order with respect to CH_4 was of 0.002, it can be concluded that there was no effect of methane presence in the feed stream on WGS rate. The apparent activation energy and the frequency factor were calculated as 28.215 kJ mol^{-1} and 29.209 μmol $mgcat^{-1}$ s^{-1} $kPa^{-0.49}$, respectively in a temperature range of 300-350 ºC.

5.2. Recommendations

Considering the results of the present study, following studies are recommended for future studies:

- FTIR-DRIFTS studies can be carried out to scrutinize the surface reactions in order to determine the plausible reaction mechanism.
- In order to investigate the effect of promoters used in Pt-Re-V/CeO_2 catalyst on the reaction kinetics, a power law type model can be obtained for Pt-Re/CeO_2 or Pt-V/CeO_2.
- Langmuir Hinshelwood Hougen-Watson type model under realistic conditions can be also investigated.
- Experiments can be performed with more than two residence times to obtain more accurate results.

REFERENCES

Aguila, G., A. Valenzuela, S. Guerrero and P. Araya, 2013, "WGS Activity of a Novel Cu–ZrO_2 Catalyst Prepared by a Reflux Method. Comparison with a Conventional Impregnation Method", Catalysis Communications, Vol. 39, pp. 82-85.

Azzam, K. G., I. V. Babich and S. L. Leffers, 2007a, "Bifunctional Catalysts for Single Stage Water–Gas Shift Reaction in Fuel Cell Applications. Part 1. Effect of the Support on the Reaction Sequence", *Journal of Catalysis,* Vol. 251, pp. 153-162.

Azzam, K. G., I. V. Babich and S. L. Leffers, 2007b, "A Bifunctional Catalyst for the Single-Stage Water–Gas Shift Reaction in Fuel Cell Applications. Part 2. Roles of the Support and Promoter on Catalyst Activity and Stability", *Journal of Catalysis,* Vol. 251, pp. 163-171.

Azzam, K. G., I. V. Babich, K. Seshan and L. Lefferts, 2008, "Role of Re in Pt-Re/TiO_2 Catalyst for Water Gas Shift Reaction: A Mechanistic and Kinetic Study", *Applied Catalysis B: Environmental,* Vol. 80, pp. 129-140.

Azzam, K. G., I. V. Babich, K. Seshan, B. L. Mojet and L. Lefferts, 2013, "Stable and Efficient Pt-Re/TiO_2 Catalysts for Water-Gas-Shift: On the Effect of Rhenium", *ChemCatChem,* Vol. 5, pp. 557-564.

Başar, M. S., 2016, *A Study on Co-Free Hydrogen Production and Adsorbent Design for Selective Carbon Dioxide Removal,* Ph.D. Thesis, Boğaziçi University.

Bunluesin, T., R. J. Gorte and G. W. Graham, 1998, "Studies of the Water-Gas Shift Reaction on Ceria-Supported Pt, Pd and Rh: Implications for Oxygen-Storage Properties", *Applied Catalysis B: Environmental,* Vol. 15, pp. 107-114.

Castano, M. G., T. R. Reina, S. Ivanova, M. A. Centeno and J. A. Odriozola, 2014, "Pt vs Au in Water–Gas Shift Reaction", *Journal of Catalysis*, Vol. 314, pp. 1-9.

Choi, Y. and H. G. Stenger, 2003, "Water Gas Shift Reaction Kinetics and Reactor Modeling for Fuel Cell Grade Hydrogen", *Journal of Power Sources*, Vol. 124, pp. 432-439.

Çağlayan, B. S. and A. E. Aksoylu, 2009. "Water-Gas Shift Reaction over Bimetallic $PtNi/Al_2O_3$ Catalysts", *Turkish Journal of Chemistry*, Vol. 33, pp. 249-256.

Çağlayan, B. S. and A. E. Aksoylu, 2011, "Water-Gas Shift Activity of Ceria Supported Au-Re Catalysts", *Catalysis Communications*, Vol. 12, pp. 1206–1211.

Demirhan, C. D., 2015, *Design and Development of WGS Catalysts for Small Scale Hydrogen Production Units*, M.S. Thesis, Boğaziçi University.

Dijk, H. A. J. van, J. Boon, R. N. Nyqvist, R. W. van den Brink, "Development of a Single Stage Heat Integrated Water–Gas Shift Reactor for Fuel Processing", *Chemical Engineering Journal*, 159, pp. 182-189.

Dönitz, W., 1998, "Fuel Cells for Mobile Applications, Status, Requirements and Future Application Potential", *International Journal of Hydrogen Energy*, Vol. 23, pp. 611-615.

Duarte de Farias, A. M., P. Bargiela, M. G. C. Rocha and M. A. Fraga, 2008, "Vanadium-Promoted Pt/CeO_2 Catalyst for Water-Gas Shift Reaction", *Journal of Catalysis*, Vol. 260, pp. 93-102.

Franchini, C. A., A. M. Duarte de Farias, E. M. Albuquerque, R. Santos and M. A. Fraga, 2012, "Single-Stage Medium Temperature Water-Gas Shift Reaction over Pt/ZrO_2–Support Structural Polymorphism and Catalyst Deactivation", *Applied Catalysis B: Environmental*, Vol. 117-118, pp. 302-309.

Germani, G., P. Alphonse, M. Courty, Y. Schuurman and C. Mirodatos, 2005, "Platinum/Ceria/Alumina Catalysts on Microstructures for Carbon Monoxide Conversion", *Catalysis Today*, Vol. 110, pp. 114-120.

Gökaliler, F., B. S. Çağlayan, Z. İ. Önsan and A. E. Aksoylu, 2008, "Hydrogen Production by Autothermal Reforming of LPG for PEM Fuel Cell Applications", *International Journal of Hydrogen Energy*, Vol. 33, pp. 1383-1391.

Gökaliler, F., Z. I. Önsan and A. E. Aksoylu, 2013, "Power-Law Type Rate Expression for WGS Reaction over Au-Re/CeO_2 Catalyst under Realistic Fuel Processor Conditions", *Catalysis Communications*, Vol. 39, pp. 70-73.

Gunawardana, P. V. D. S., H. C. Lee and D. H. Kim, 2009, "Performance of Copper–Ceria Catalysts for Water Gas Shift Reaction in Medium Temperature Range", *International Journal of Hydrogen Energy*, Vol. 34, pp. 1336-1341.

Guo, P. J., L. F. Chen, G. B. Yu, Y. Zhu, M. H. Qiao, H. L. Xu and K. N. Fan, 2009, "Cu/ZnO-Based Water-Gas Shift Catalysts in Shut-down/Start-up Operation", *Catalysis Communications*, Vol. 10, pp. 1252-1256.

Haber, J., M. Witko and R. Tokartz, 1997, "Vanadium Pentoxide I. Structures and Properties", *Applied Catalysis*, Vol. 157, pp. 3-22.

Hilaire, S., X. Wang, T. Luo, R. J. Gorte and J. Wagner, 2001, "A Comparative Study of Water-Gas-Shift Reaction over Ceria Supported Metallic Catalysts", *Applied Catalysis A: General*, Vol. 215, pp. 271-278.

Hla, S. S., D. Park, G. J. Duffy, J. H. Edwards, D. G. Roberts, A. Ilyushechkin, L. D. Morpeth and T. Nguyen, 2009, "Kinetics of High Temperature Water-Gas Shift Reaction over Two Iron-Based Commercial Catalyst Using Simulated Coal-Derived Syngases", *Chemical Engineering Journal*, Vol. 146, pp. 148-154.

Holladay, J. D. and Y. Wang, 2015, "A Review of Recent Advances in Numerical Simulations of Microscale Fuel Processor for Hydrogen Production", *Journal of Power Sources*, Vol. 282, pp. 602-621.

Hu, Y. H. and E. Ruckenstein, 2004, "Catalytic Conversion of Methane to Synthesis Gas by Partial Oxidation and CO_2 Reforming", *Advances in Catalysis*, Vol. 48, pp. 297-345.

Jacobs, G., L. Williams, U. Graham, D. Sparks and B. H. Davis, 2003, "Low-Temperature Water-Gas Shift: In-Situ DRIFTS-Reaction Study of a Pt/CeO_2 Catalyst for Fuel Cell Reformer Applications", *Journal of Physical Chemistry B*, Vol. 107, pp. 10398-10404.

Kalamaras, C. M., P. Panagiotopoulou, D. I. Kondarides and A. M. Efstathiou, 2009, "Kinetic and Mechanistic Studies of the Water-Gas Shift Reaction on Pt/TiO_2 Catalyst", *Journal of Catalysis*, Vol. 264, pp. 117-129.

Kalamaras, C. M., S. Americanou and A. M. Efstathiou, 2011, "Redox vs Associative Formate with –OH Group Regeneration WGS Reaction Mechanism on Pt/CeO_2: Effect of Platinum Particle Size", *Journal of Catalysis*, Vol. 279, pp. 287-300.

Kam, R., J. Scott, R. Amal and C. Selomulya, 2010, "Pyrophoricity and Stability of Copper and Platinum Based Water-Gas Shift Catalysts during Oxidative Shut-down/Start-up Operation", *Chemical Engineering Science*, Vol. 65, pp. 6461-6470.

Keiski, R. L., T. Salmi and V. J. Pohjola, 1992, "Development and Verification of a Simulation Model for a Non-Isothermal Water-Gas Shift Reactor", *The Chemical Engineering Journal*, Vol. 48, pp. 17-29.

Keiski, R. L., T. Salmi, P. Niemesto, J. Ainassaari and V. J. Pohjola, 1996, "Stationary and Transient Kinetics of the High Temperature Water-Gas Shift Reaction", *Applied Catalysis A: General*, Vol. 137, pp. 349-370.

Kesim, B., 2017, *An Experimental Study on Optimization of Pt-Based Trimetallic WGS Catalysts*, M.S. Thesis, Boğaziçi University.

Kolb, G., 2008, *Fuel Processing for Fuel Cells*, first ed., Wiley, Weinheim.

Krekel, D., Samsun, R. C., Pasel, J., Prawitz, M., Peters, R. and Stolten, D., 2016, "Operating Strategies for Fuel Processing Systems with a Focus on Water–Gas Shift Reactor Stability", *Applied Energy*, Vol. 164, pp. 540-552.

Koryabkina, N. A., A. A. Phatak, W. F. Ruettinger, R. J. Farrauto and F. H. Riberio, 2003, "Determination of Kinetic Parameters for the Water-Gas Shift Reaction on Copper Catalysts under Realistic Conditions for Fuel Cell Applications", *Journal of Catalysis*, Vol. 217, pp. 233-239.

Lenite, B. A., C. Galletti and S. Specchia, 2011, "Studies on Au Catalysts for Water Gas Shift Reaction", *International Journal of Hydrogen Energy*, Vol. 26, pp. 7750-7758.

Leppelt, R., B. Schumacher, V. Plzak, M. Kinne and R. J. Behm, 2006, "Kinetics and Mechanism of the Low-Temperature Water-Gas Shift Reaction on Au/CeO_2 Catalysts in an Idealized Reaction Atmosphere", *Journal of Catalysis*, Vol. 244, pp. 137-152.

LeValley, T. L., A. R. Richard and M. Fan, 2014, "The Progress in Water Gas Shift and Steam Reforming Hydrogen Production Technologies-A Review", *International Journal of Hydrogen Energy*, Vol. 39, pp. 16983-17000.

Liu, X., W. Ruettinger, X. Xu and R. Farrauto, 2005, "Deactivation of Pt/CeO_2 Water-Gas Shift Catalysts due to Shutdown/Startup Modes for Fuel Cell Applications", *Applied Catalysis B: Environmental*, Vol. 56, pp. 69-75.

Liu, X., P. Guo, S. Xie, Y. Pei, M. Qiao and K. Fan, 2012, "Effect of Cu Loading on Cu/ZnO Water-Gas Shift Catalysts for Shut-down/Start-up Operation", *International Journal of Hydrogen Energy*, Vol. 37, pp. 6381-6388.

Liu, X., P. Guo, B. Wang, Z. Jiang, Y. Pei, K. Fan and M. Qiao, 2013, "A Comparative Study of the Deactivation Mechanisms of the Au/CeO_2 Catalyst for Water–Gas Shift under Steady-State and Shut-down/Start-up Conditions in Realistic Reformate", *Journal of Catalysis*, Vol. 300, pp. 152-162.

Mhadeshwar, A. B. and D. G. Vlachos, 2005, "Is the Water–Gas Shift Reaction on Pt simple? Computer-Aided Microkinetic Model Reduction, Lumped Rate Expression, and Rate Determining Step", *Catalysis Today*, Vol. 105, pp. 162-172.

Mond L. and C. Langer, 1888, "Improvements in Obtaining Hydrogen", *British Patent*, 12608.

Nguyen-Thanh, D., A. M. Duarte de Farias and M. A. Fraga, 2008, "Characterization and Activity of Vanadia-Promoted Pt/ZrO_2 Catalysts for the Water-Gas Shift Reaction", *Catalysis Today*, Vol. 138, pp. 235-238.

Nishimura, S., T. Shishido, K. Ebitani, K. Teramura and T. Tanaka, 2010, "Novel Catalytic Behavior of Cu/Al_2O_3 Catalyst against Daily Start-up and Shut-down (DSS)-like Operation in the Water Gas Shift Reaction", *Applied Catalyst A: General*, Vol. 387, pp. 185-194.

Ogden, J. M., 1999, "Prospects for Building a Hydrogen Energy Infrastructure", *Annual Review of Energy and the Environment*, Vol. 24, pp. 227–79.

O'Hayre, R., S. W. Cha, W. Colella and F. B. Prinz, 2009, "*Fuel Cell Fundamentals"*, second ed., Wiley, New York.

Okada, O. and K. Yokoyama, 2001, "Development of Polymer Electrolyte Fuel Cell Cogeneration Systems for Residential Applications", Vol. 1, pp. 72-77.

Ovesen, C. V., P. Stoltze, J. K. Norskov and C. T. Campbell, 1992, "A Kinetic Model of the Water Gas Shift Reaction", *Journal of Catalysis*, Vol. 134, pp. 445-468.

Ovesen, C. V., B. S. Clausen, B. S. Hammershoi, G. Steffensen, T. Askgaard, I. Chorkendorff, J. K. Norskov, P. B. Rasmussen, P. Stoltze and P. Taylor, 1996, "A Microkinetic Analysis of the Water-Gas Shift Reaction under Industrial Conditions", *Journal of Catalysis*, Vol. 158, pp. 170-180.

Perez, L. P., R. B. Sierra and A. S. Escribano, 2014, "CeO_2-Promoted Ni/Activated Carbon Catalysts for the Water-Gas Shift (WGS) Reaction", *International Journal of Hydrogen Energy*, Vol. 39, pp. 17589-17599.

Phatak, A. A., N. Koryabkina, S. Rai, J. L. Ratts, W. Ruettinger, R. J. Farrauto, G. E. Blau and W. N. Delgass, 2007, "Kinetics of the Water-Gas Shift Reaction on Pt Catalysts Supported on Alumina and Ceria", *Catalysis Today*, Vol. 123, pp. 224-234.

Plaza, A., S. Fail, J. A. Cortes, K. Föttinger, N. Diaz, R. Rauch and H. Hofbauer, 2016, "Apparent Kinetics of the Catalyzed Water–Gas Shift Reaction in Synthetic Wood Gas", *Chemical Engineering Journal*, Vol. 301, pp. 222-228.

Pradhan, S., A. S. Reddy, R. N. Devi and S. Chilukuri, 2009, "Copper-Based Catalysts for Water Gas Shift Reaction: Influence of Support on Their Catalytic Activity", *Catalysis Today*, Vol. 141, pp. 72- 76.

Radhakrishnan, R., R. R. Willigan, Z. Dardas and T. H. Vanderspurt, 2006, "Water Gas Shift Activity and Kinetics of Pt/Re Catalysts Supported on Ceria-Zirconia Oxides", *Applied Catalysis B: Environmental*, Vol. 66, pp. 23-28.

Ratnasamy, P., D. Srinivas, C. V. V. Satyanarayana, P. Manikandan, R. S. S. Kumaran, M. Sachin and V. N. Shetti, 2004, "Influence of the Support on the Preferential Oxidation of CO in Hydrogen-Rich Steam Reformates over the $CuO–CeO_2–ZrO_2$ System", *Journal of Catalysis*, Vol. 221, pp. 455-465.

Reina, T. R., S. Ivanova, M. A. Centeno and J. A. Odriozola, 2015, "Boosting the Activity of $Au/CeO_2/Al_2O_3$ Catalyst for the WGS Reaction", *Catalysis Today*, Vol. 253, pp. 149-154.

Reina, T. R., S. Ivanova, M. A. Centeno and J. A. Odriozola, 2016, "The Role of Au, Cu & CeO_2 and Their Interactions for an Enhanced WGS Performance", *Applied Catalysis B: Environmental*, Vol. 187, pp. 98-107.

Roh, H. S., D. W. Jeong, K. S. Kim, I. H. Eum, K. Y. Koo, W. L. Yoon, 2011, "Single Stage Water-Gas Shift Reaction Over Supported Pt Catalysts", *Catalysis Letters*, Vol. 141, pp. 95-99.

Rostrup-Nielsen, J. R., 1984, "Sulfur-Passivated Nickel Catalysts for Carbon-free Steam Reforming of Methane", *Journal of Catalysis*, Vol. 85, pp. 31-43.

Sathre, R., 2014, "Comparing the Heat of Combustion of Fossil Fuels to the Heat Accumulated by Their Lifecycle Greenhouse Gases", *Fuel*, Vol. 115, pp. 674-677.

Smith, B. R. J., M. Loganathan and M. S. Shantha, 2010, "A Review of Water Gas Shift Reaction Kinetics", *International Journal of Chemical Reactor Engineering*, Vol. 8, pp. 1-32.

Shekhawat, D., J. J. Spivey and D. A. Berry, 2011, "*Fuel Cells: Technologies for Fuel Processing*", Elsevier, Oxford, UK.

Tepematr, P., N. Laosiripojana and S. Charojrochkul, 2016, "Water Gas Shift Reaction over Monometallic and Bimetallic Catalysts Supported by Mixed Oxide Materials", *Applied Catalysis A: General*, Vol. 523, pp. 255-262.

Trimm, D. L. and Z. İ. Önsan, 2001, "Onboard Fuel Conversion Hydrogen-Fuel-Cell-Driven Vehicles", *Catalysis Reviews: Science and Engineering*, Vol. 43, pp. 31-84.

Villar, V., L. Barrio, A. Helmi, M. S. Annaland, F. Gallucci, J. L. G. Fierro and R. M. Navarro, 2016, "Effect of Re Addition on the WGS Activity and Stability of Pt/CeO_2–TiO_2 Catalyst for Membrane Reactor Applications", *Catalysis Today*, Vol. 268, pp. 95–102.

Zhu, X., M. Shen, L. L. Lobban and R. G. Mallinson, 2011, "Structural Effects of Na Promotion for High Water Gas Shift Activity on Pt-Na/TiO_2", *Journal of Catalysis*, Vol. 278, pp. 123–132.

APPENDIX A: CONVERSION VERSUS RESIDENCE TIME GRAPHS

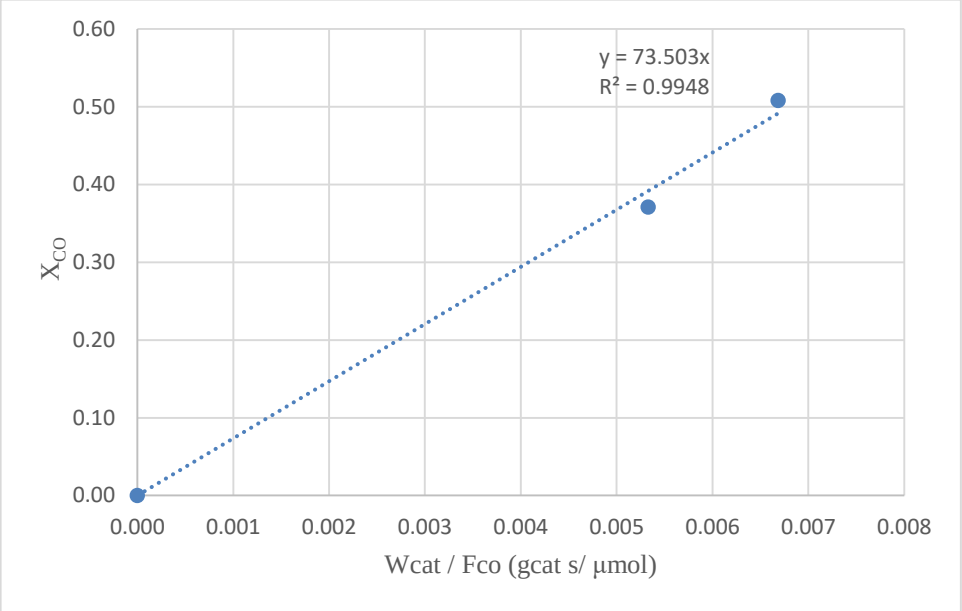

Figure A.1. Fractional CO conversion vs. residence time graph for Run 1a-1b.

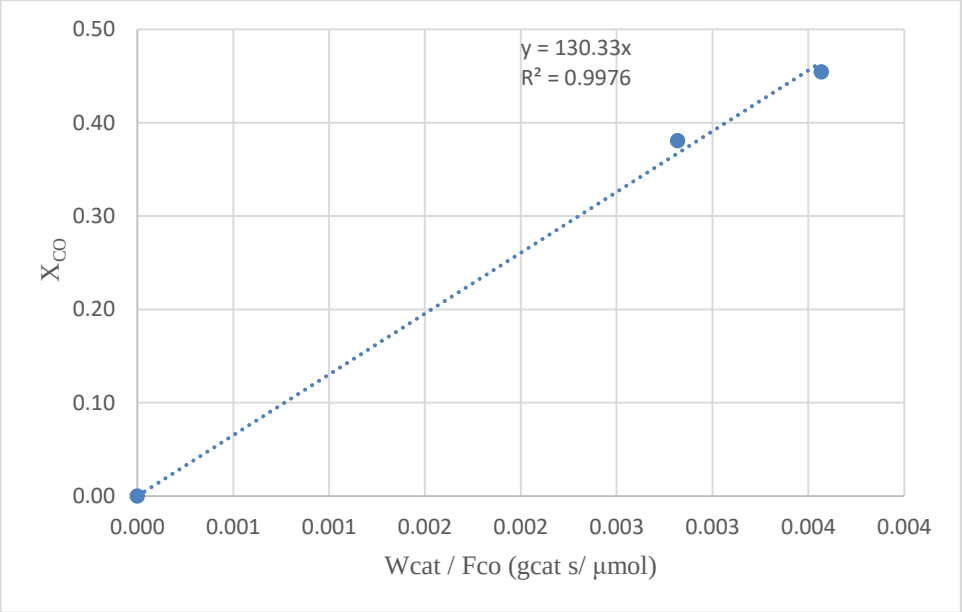

Figure A.2. Fractional CO conversion vs. residence time graph for Run 2a-2b.

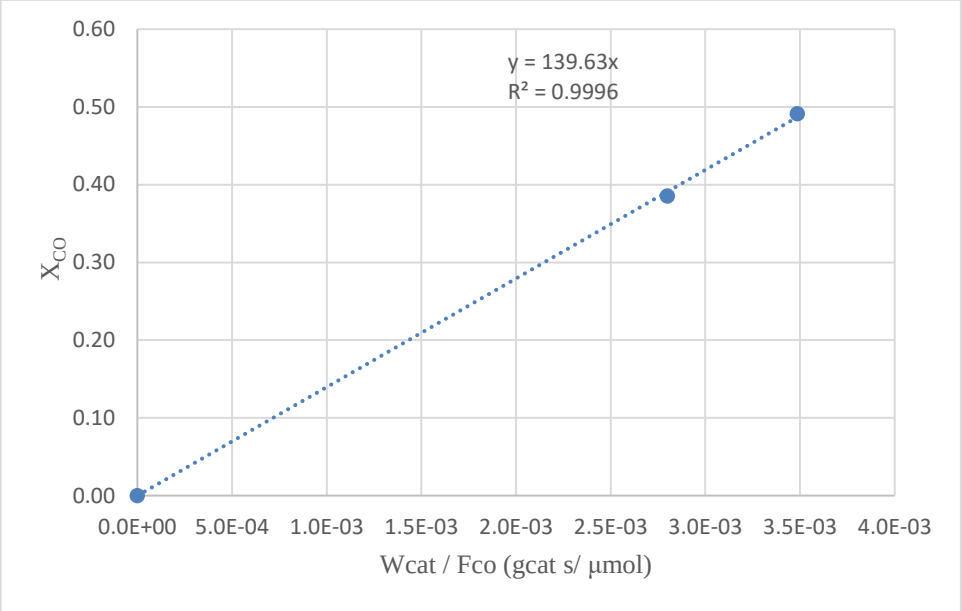

Figure A.3. Fractional CO conversion vs. residence time graph for repeated Run 2a-2b.

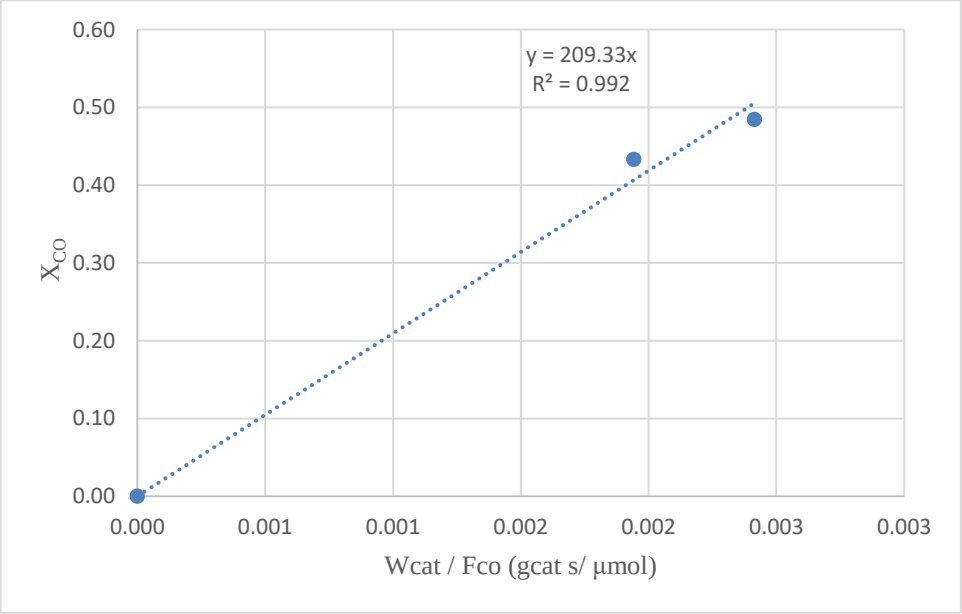

Figure A.4. Fractional CO conversion vs. residence time graph for Run 3a-3b.

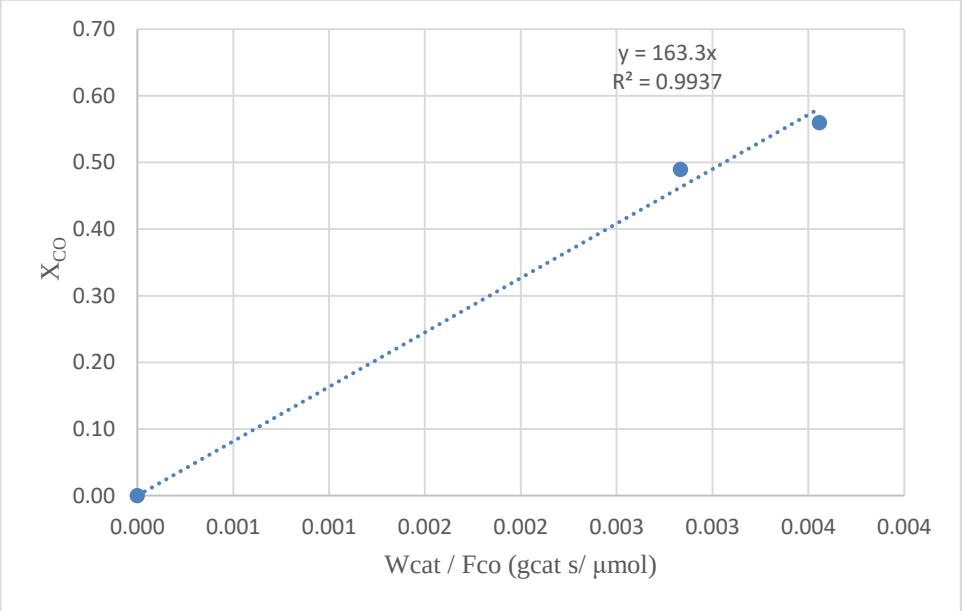

Figure A.5. Fractional CO conversion vs. residence time graph for Run 4a-4b.

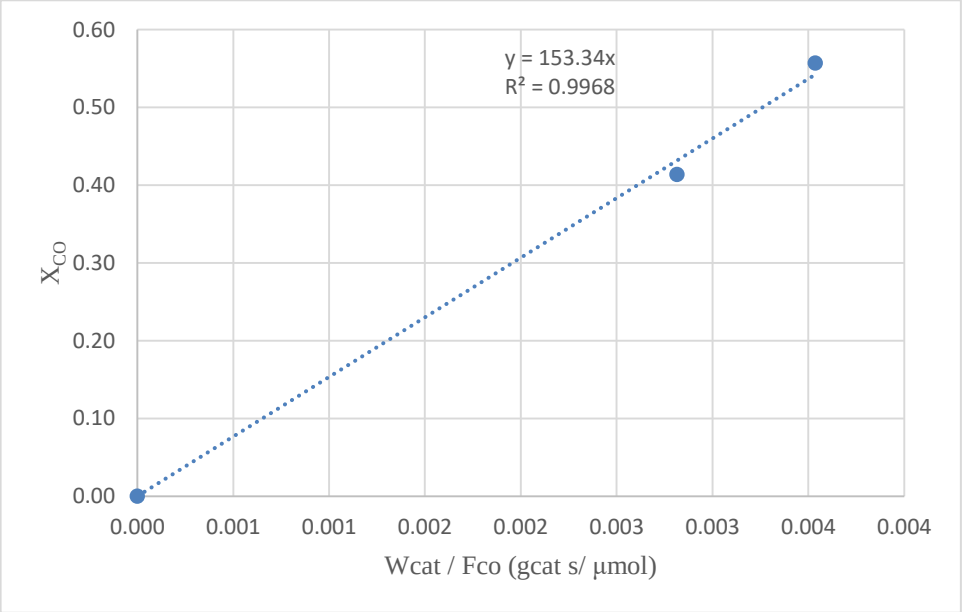

Figure A.6. Fractional CO conversion vs. residence time graph for Run 5a-5b.

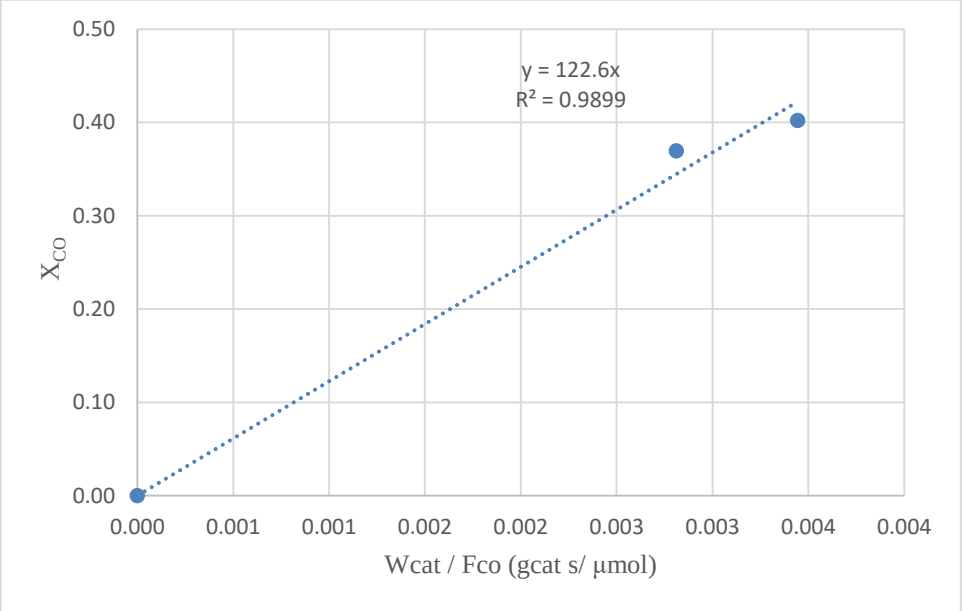

Figure A.7. Fractional CO conversion vs. residence time graph for Run 6a-6b.

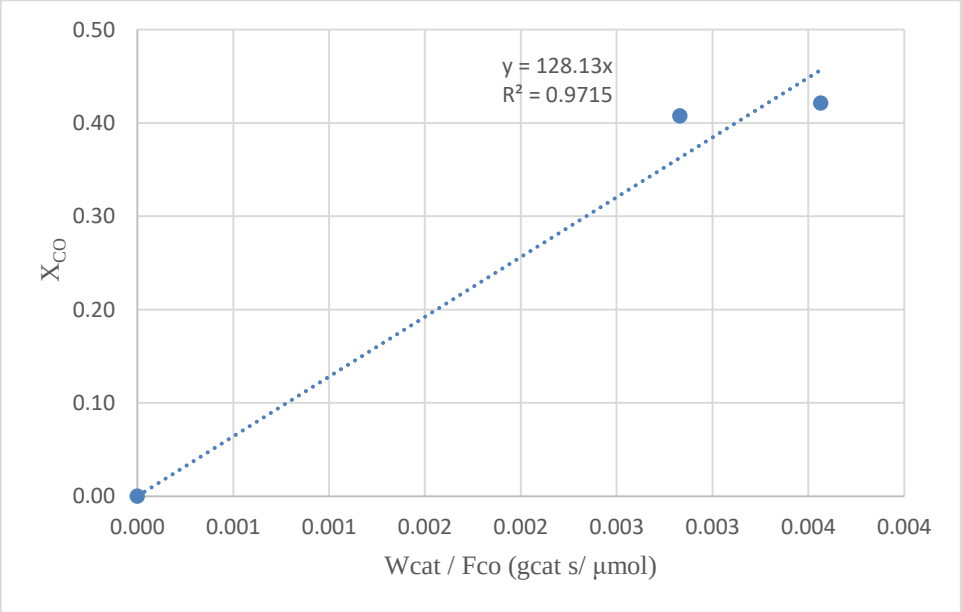

Figure A.8. Fractional CO conversion vs. residence time graph for Run 7a-7b.

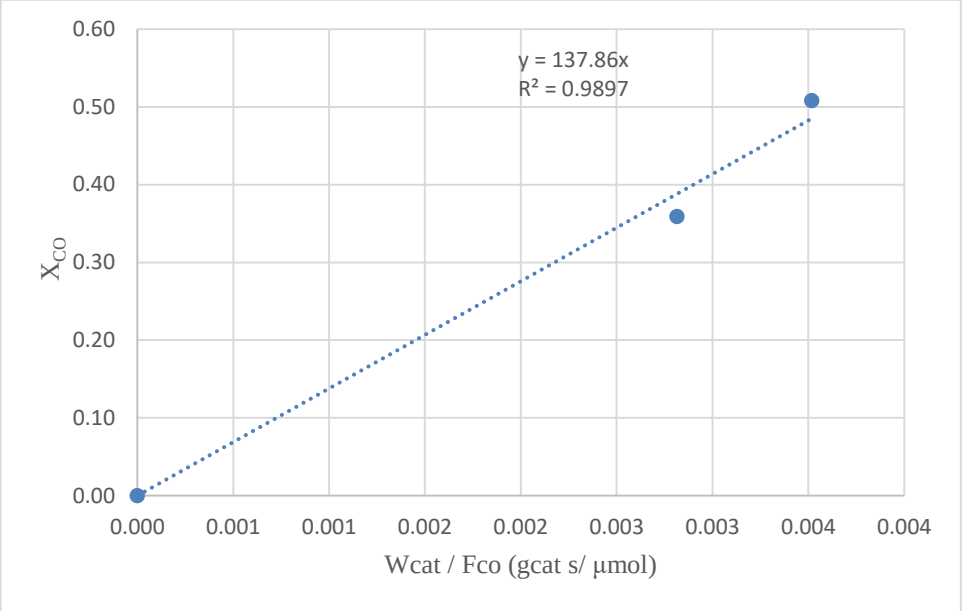

Figure A.9. Fractional CO conversion vs. residence time graph for Run 8a-8b.

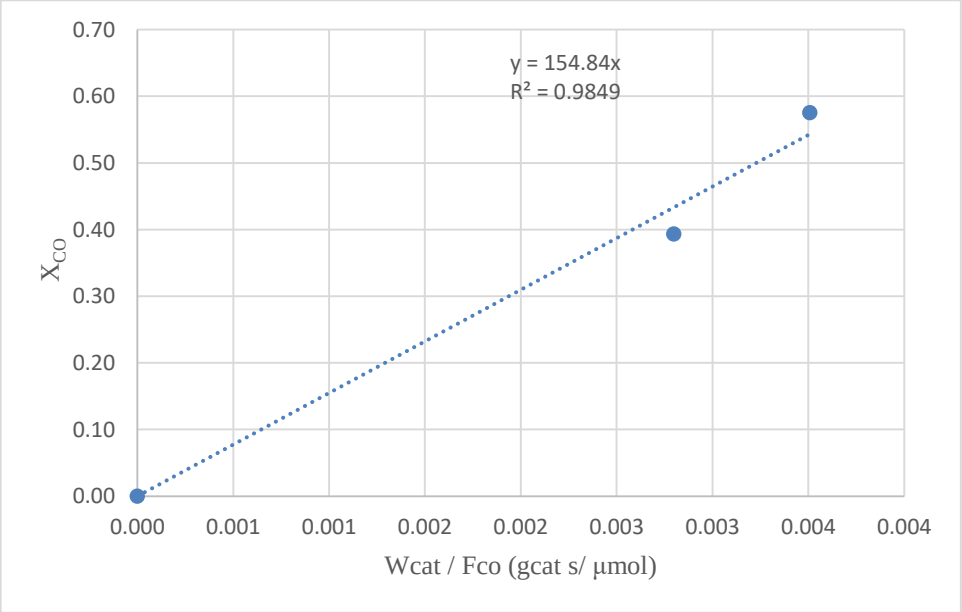

Figure A.10. Fractional CO conversion vs. residence time graph for Run 9a-9b.

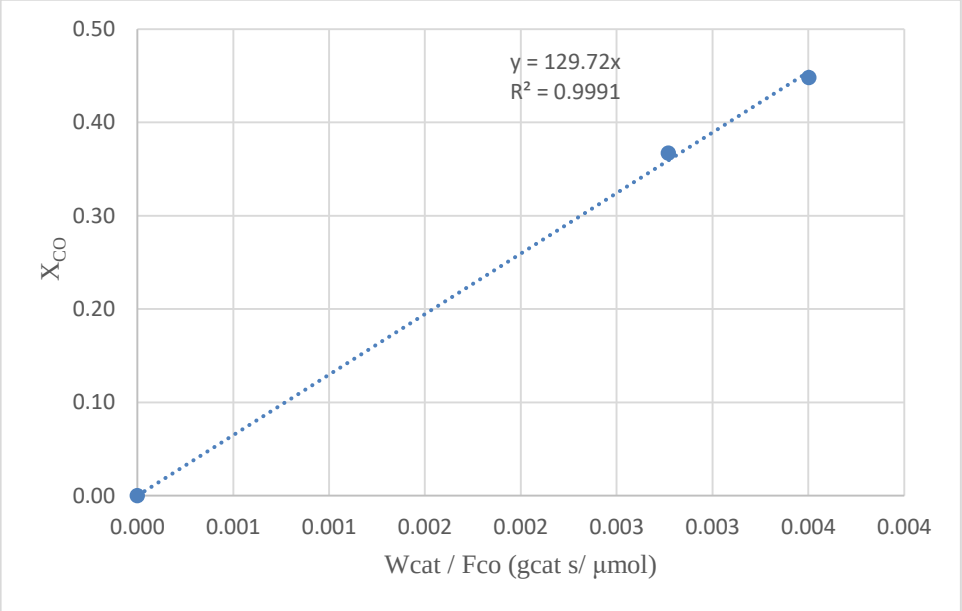

Figure A.11. Fractional CO conversion vs. residence time graph for Run 10a-10b.

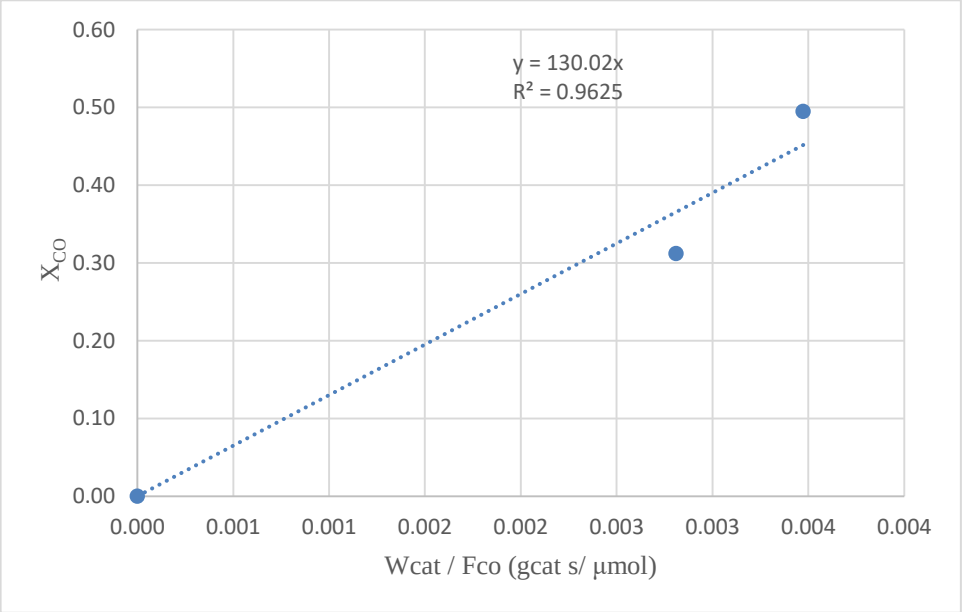

Figure A.12. Fractional CO conversion vs. residence time graph for Run 11a-11b.

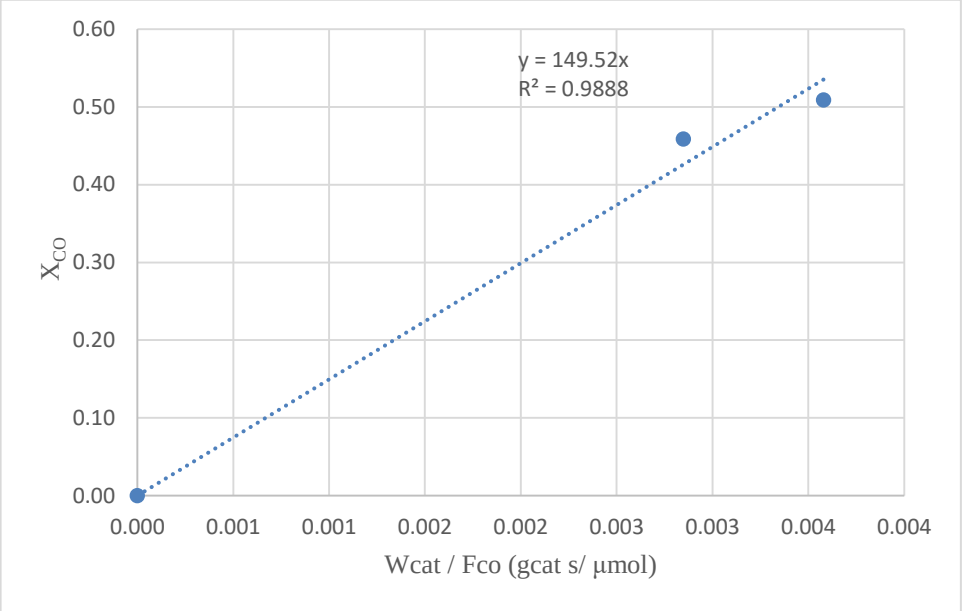

Figure A.13. Fractional CO conversion vs. residence time graph for Run 12a-12b.

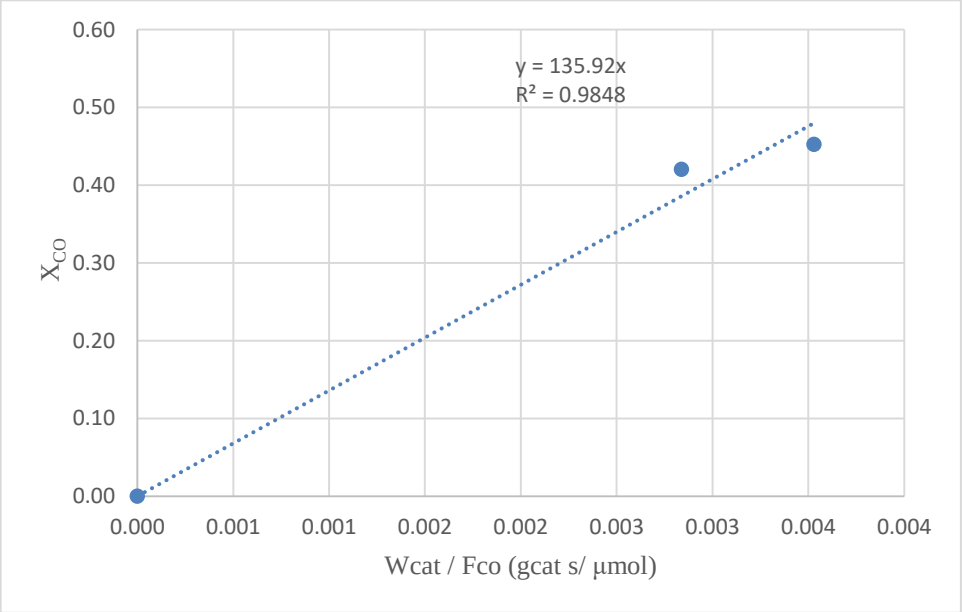

Figure A.14. Fractional CO conversion vs. residence time graph for Run 13a-13b.

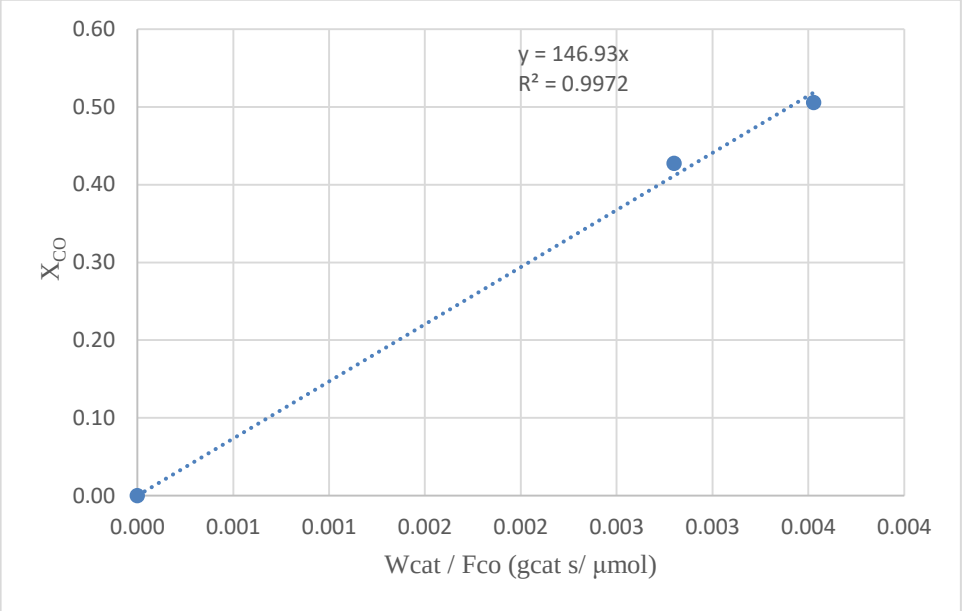

Figure A.15. Fractional CO conversion vs. residence time graph for Run 14a-14b.

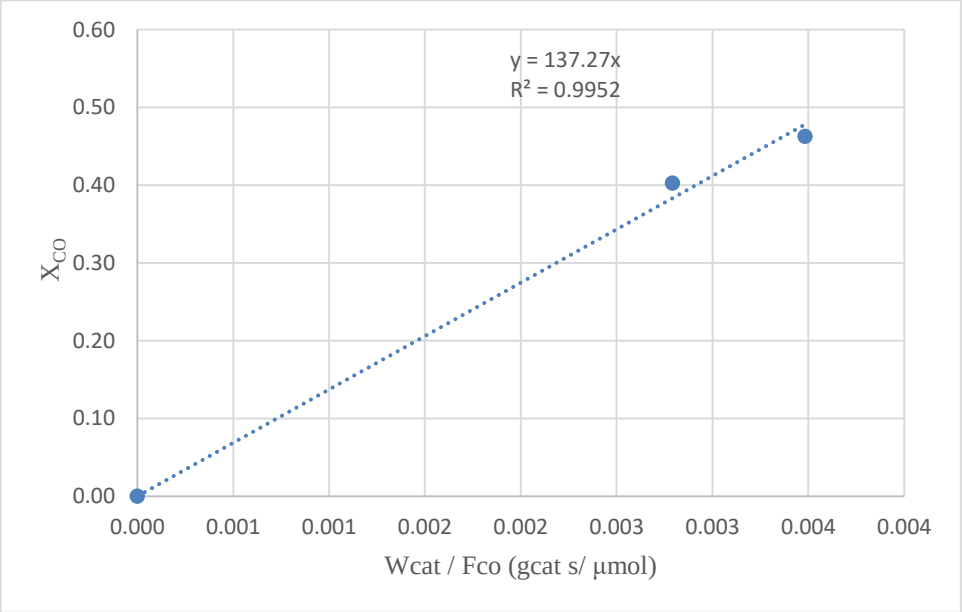

Figure A.16. Fractional CO conversion vs. residence time graph for Run 15a-15b.

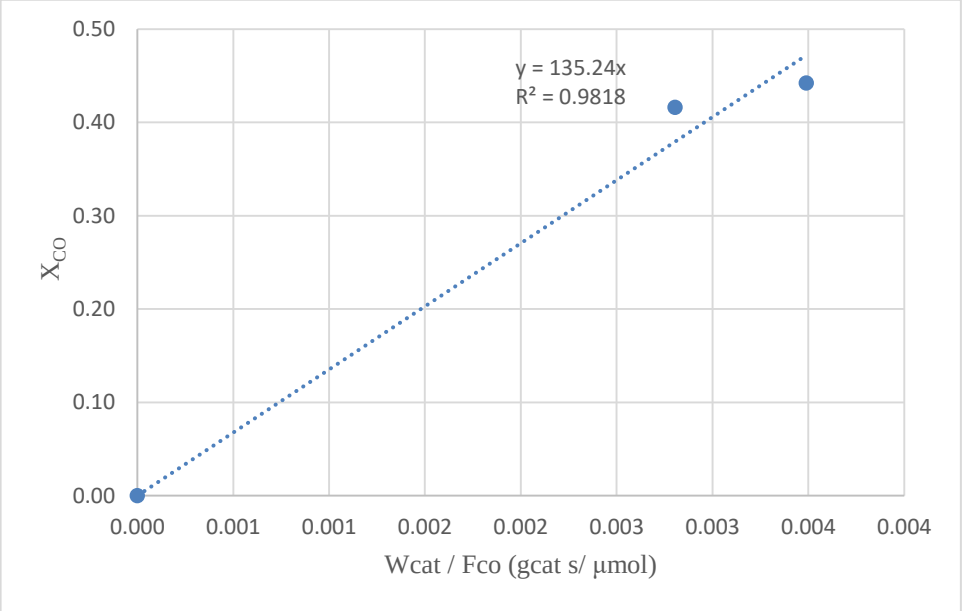

Figure A.17. Fractional CO conversion vs. residence time graph for Run 16a-16b.

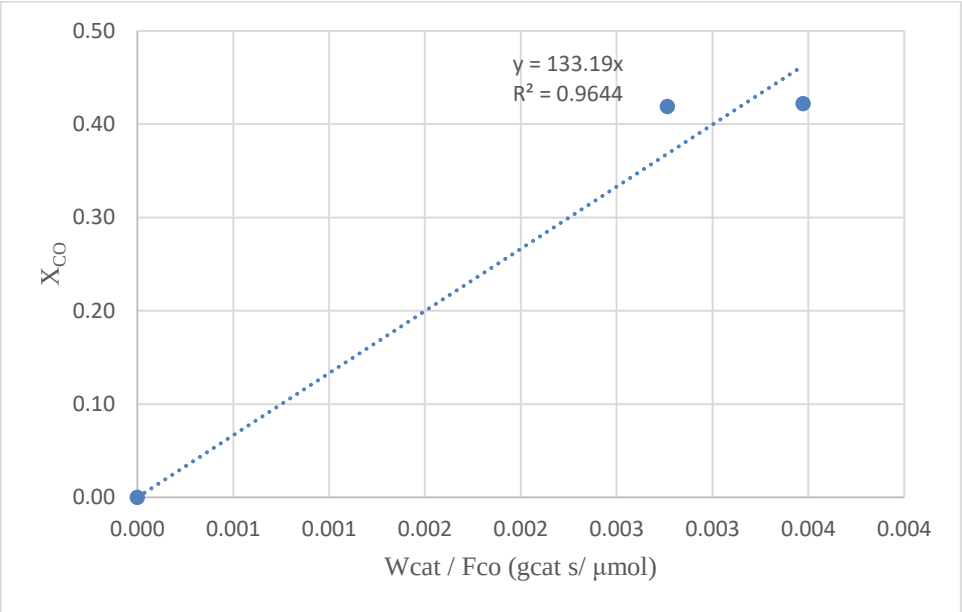

Figure A.18. Fractional CO conversion vs. residence time graph for Run 17a-17b.